Beatriz Gonçalves Crisóstomo Esteves

Bachelor of Science in Biomedical Engineering

Personality assessment based on biosignals during a decision-making task

Dissertation submitted in partial fulfillment
of the requirements for the degree of

Master of Science in
Biomedical Engineering

Adviser: Prof. Doctor Hugo Gamboa, Auxiliar Professor, NOVA University of Lisbon

Co-adviser: Prof. Doctor Marcus Cheetham, Full Professor, Nungin University, and Senior Research Associate, University of Zurich

FACULDADE DE CIÊNCIAS E TECNOLOGIA
UNIVERSIDADE NOVA DE LISBOA

October, 2017

Personality assessment based on biosignals during a decision-making task

This document was created using the (pdf)LaTeX processor, based in the "unlthesis" template[1], developed at the Dep. Informática of FCT-NOVA [2].
[1] https://github.com/joaomlourenco/unlthesis [2] http://www.di.fct.unl.pt

Acknowledgements

Primeiro gostaria de agradecer ao Professor Hugo Gamboa, pela oportunidade que me deu em poder participar num projecto tão desafiante e que se revelou ao longo destes meses cada vez mais interessante. Os seus constantes conselhos e desafios foram muito importantes para o desenvolvimento do meu trabalho. Também tenho de agradecer ao Professor Marcus Cheetham, pela motivação e disponibilidade para discutir temas de psicologia e os resultados que fomos obtendo ao longo desta tese. Gostaria também de agradecer ao Departamento de Psicologia da Universidade de Zurique pela disponibilização dos dados. Não posso deixar de agradecer à Cátia Cepeda por todos os conselhos que me deu ao longo da realização da tese e por estar sempre disponível para esclarecer as minhas dúvidas e para discutir novos resultados.

Estou também agradecida à minha família por terem investido em mim e por me terem dado a oportunidade de estudar este curso. Agradeço aos meus pais, irmão e avós por acreditarem em mim e pela força que me deram em todas as etapas. À minha madrinha por estar sempre presente na minha vida, me ter dado a oportunidade de fazer parte da vida dos meus dois meninos, Guilherme e Afonso, e muito, muito mais. Obrigada por todo o apoio.

Por fim, agradeço a todas as amizades que passaram na minha vida nestes últimos 6 anos e que tornaram todo o estudo muito mais fácil com os momentos de diversão. À minha equipa que me proporcionou momentos de descontração e de orgulho que nunca esquecerei. À minha *personal assistent* Carina Figueiredo por estar sempre lá para mim e nunca me deixar desistir, não conseguia sem ti. Muito, muito obrigada.

Abstract

Due to the emergence of novel acquisition devices and signal processing techniques, the study of electrophysiology and its applications has assumed an important role on the Biomedical Engineering community. Recently, research on this area has expanded to several domains, with the psychophysiology being a proeminent one, more specifically in the field of personality psychology.

In this thesis, participants were asked to perform a wildly known decision-making task, the Iowa Gambling Task (IGT), and their biosignals were recorded during this performance with the objective of determining whether changes in biosignals could be related to personality. This project was composed by 71 participants and their biosignals were used to extract meaningful features that together could create a predictive model of personality. For this, all biosignals were processed prior to the feature extraction step and the features were extracted from the entire signals, recorded during the performance of the IGT, and also dividing the task in five blocks. After the extraction, a machine learning algorithm was used to compute the best predictive models for the Five Factor Model (FFM) personality dimensions and for the Maximization and Regret scales, using each biosignal individually and in the end all features from all biosignals.

The results showed that the predictive models which use features from all biosignals perform better than the models which use only one biosignal. The Openness to Experience, Agreeableness and Maximization scales are well predicted with features from Electrocardiogram (ECG), the Agreeableness, Maximization and Extraversion scales with Electrodermal Activity (EDA) features and the Extraversion and Openness to Experience scales with features from Blood Volume Pulse (BVP). The hypothesis that personality traits is more expressed in the start of IGT was confirmed since the highest number of features is extracted from the Block 1 of the IGT. The results should be further validated for other populations.

Keywords: Biosignals, Signal Processing, Feature Selection, Machine Learning, Iowa Gambling Task, Five Factor Model, Maximization

Resumo

Devido ao aparecimento de novos dispositivos de aquisição e técnicas de processamento de sinais, o estudo da eletrofisiologia e das suas aplicações assumiu um papel importante na comunidade de Engenharia Biomédica. Recentemente, a pesquisa nesta área expandiu-se para várias áreas, sendo uma das mais proeminentes a psicofisiologia, mais especificamente na área da psicologia da personalidade.

Nesta tese, os participantes foram convidados a realizar uma tarefa de tomada de decisão extremamente conhecida, o IGT, e os seus biosinais foram registados durante esta performance com o objetivo de determinar se mudanças nas características dos biosinais poderiam estar relacionadas com a personalidade. Este projeto teve a participação de 71 participantes e os seus biosinais foram utilizados para extrair características significativas que em conjunto poderiam criar um modelo preditivo de personalidade. Para isso, todos os biosinais foram processados antes de se proceder à extração de parâmetros dos sinais e os parâmetros foram extraídos dos sinais completos, registados durante a performance do IGT, assim como da divisão do jogo em cinco blocos. Após a extração, um algoritmo de aprendizagem automática foi utilizado para determinar os melhores modelos preditivos para as dimensões da personalidade do modelo dos cinco fatores e para as escalas de Maximização e Arrependimento, usando cada biosinal individualmente e por fim a combinação de todos os parâmetros de todos os biosinais.

Os resultados mostraram que os modelos preditivos que utilizam características de todos os biosinais são melhores do que os modelos que utilizam apenas um biosinal. As escalas *Abertura à Experiência*, *Amabilidade* e *Maximização* são bem previstas através de parâmetros do eletrocardiograma (ECG), as escalas *Amabilidade*, *Maximização* e *Extroversão* através do atividade eletrodérmica (EDA) e as escalas *Extroversão* e *Abertura à Experiência* através do volume de pulso sanguíneo (BVP). A hipótese de que a personalidade é mais expressa no início do IGT foi confirmada uma vez que o maior número de parâmetros dos sinais é extraído do primeiro bloco do IGT. Estes resultados devem ser validados para outras populações.

Palavras-chave: Biosinais, Processamento de Sinais, Seleção de parâmetros, Aprendizagem Automática, Iowa Gambling Task, Modelo dos Cinco Fatores, Maximização

Contents

List of Figures

List of Tables

Acronyms

ACC	Anterior Cingulate Cortex.
ADC	Analog-to-Digital Converter.
ANS	Autonomic Nervous System.
ApEn	Approximate Entropy.
AUC	Area Under the Curve.
BAV	BVP peak-to-peak Amplitude Variation.
bpm	beats per minute.
BVP	Blood Volume Pulse.
CD	Correlation dimension.
CNS	Central Nervous System.
DFA	Detrended Fluctuation Analysis.
DLPFC	Dorsolateral Prefrontal Cortex.
ECG	Electrocardiogram.
EDA	Electrodermal Activity.
EEG	Electroencephalogram.

ER-SCR	Event Related Skin Conductance Responses.
ETG	Eye Tracking Glasses.
FD	Fractal Dimension.
FFM	Five Factor Model.
fs	sampling frequency.
HCI	Human–Computer Interaction.
HF	Power in High Frequencies.
HR	Heart Rate.
HRV	Heart Rate Variability.
Hurst	Hurst Exponent.
IBI	Interbeat Interval.
IGT	Iowa Gambling Task.
LF	Power in Low Frequencies.
LF/HF	Ratio between Low and High Frequencies.
LLE	Largest Lyapunov Exponent.
M	Mean.
MEG	Magnetoencephalogram.
NC	normal control.

NEO-FFI	NEO Five-Factor Inventory.
NEO-PI-R	Revised NEO Personality Inventory.
NN50	Number of pairs of successive NN intervals that differ by more than 50 ms.
NS-SCR	Non-Specific Skin Conductance Responses.
OFC	Orbitofrontal Cortex.
OLS	Ordinary Least Squares.
PG	pathological gamblers.
pNN50	Percentage of NN differences greater than 50 ms.
PNS	Peripheral Nervous System.
PPG	Photoplethysmographic.
PS	physiological signals.
PSD	Power Spectrum Density.
PSNS	Parasympathetic Nervous System.
RED	Remote Eye tracking Devices.
RMSD	Root Mean Squared Deviation.
RMSSD	Root Mean Square of Successive period Differences.
SampEn	Sample Entropy.
SCL	Skin Conductance Level.

SCR	Skin Conductance Responses.
SD	Standard Deviation.
SD1	Standard Deviation of instantaneous beat-to-beat variability.
SD1/SD2	Ratio of short interval variation to long interval variation.
SD2	Long-term Standard Deviation of continuous NN intervals.
SDNN	Standard Deviation of the NN interval (beat to beat interval).
SMI	SensoMotoric Instruments.
SNS	Sympathetic Nervous System.
SoNS	Somatic Nervous System.
SSF	Slope Sum Function.
TINN	Triangular Interpolation of the NN intervals.
VMPFC	Ventromedial Prefrontal Cortex.

Chapter 1

Introduction

1.1 Context

Whether in the field of biomechanics, tissue engineering or biosignal processing, biomedical engineering research has brought powerful and important tools that connect technology with biology and medicine.

The emergence of new signal processing techniques and more sophisticated acquisition devices and sensors has improved knowledge about electrophysiological signals and their applications, for example in the diagnosis of diseases or in the improvement of athletes' performance. Recently the field of psychophysiology has been extensively explored and biomedical engineering can offer an important support in this area, especially in the study of the physiological changes.

With the development of this thesis, the acquirement of biosignals, such as ECG, BVP, pupillometry and EDA, during the performance of a gambling task that simulates real life decision making, will be correlated with the FFM personality traits and the Maximization and Regret scales to test a possible correlation between the latter and features extracted from the biosignals. For this study, the IGT will be used to simulate real-life decision making. This task is a card game that simulates decision making in a environment where the player receives feedback after each round and in the long run they should conclude that the card decks associated with a high gain are associated with a high loss and the card decks with low gain are associated with a low loss, so the latter are more advantageous.

Decision making is a complex and dynamic process that is influenced by many factors, such as personality, stress or social environment. The personality trait perspective is of particular interest to study because it can be easily related to the resources used by a person to search for information in order to make a decision. Personality can have an impact in several steps of the decision making process, such as the recognition of the

problem or the selection of the best alternative to solve it.

This could also be an improvement in the field of psychology since if we could correlate features extracted from biosignals with personality traits, we could start to classify a subject as a neurotic person based on their biosignals instead of using the standard personality questionnaires. This classification based on the biosignals can avoid the cases where the subjects are not truthful when answering the questions.

In this way, this work can help individuals to understand the impact of their personality on their decision making performance. For example, this can have a big impact on manage doctors and human resources since hospitals generally prefer individuals who are quick and efficient to decide on the diagnosis and treatment of patients.

The main goal of this thesis is to find a relation between specific personality traits and the behaviour expressed during the performance of the IGT. These patterns of decision making behaviour will be collected, along with physiological signals, and will be classified by a machine learning algorithm. To do this, after being acquired, the biosignals will be processed with the goal of extracting significant features that can be used to construct a prediction model that with the extracted features can predict personality and decision making behavior results given by well known and validated questionnaires.

This dissertation work was developed in Faculdade de Ciências e Tecnologia - Universidade Nova de Lisboa and also in colaboration with the Department of Psychology of the University of Zurich, which provided the participants and the experimental conditions needed to record their data for the development of this project.

1.2 Theoretical Concepts

In this section some theoretical concepts, essential for the understanding of this work, are introduced. Firstly it is given an introduction to the nervous system and also to the biosignals that will be measured while the participant is performing the IGT and then are processed to extract different features. Then an explanation about human-computer interaction and its importance in today's world is given. Next there is a definition of personality and the FFM theory is explored. And, finally, it is introduced one of the key concepts of this work, the decision making behaviour explained by the theory of maximizers and satisficers.

1.2.1 Nervous System

The way we act, behave and even the way our body works depends on two complex and organized regulatory systems, the nervous system and the endocrine system. The nervous system is composed by a network of neurons that works sending electrical signals that control the responses of our body. This system comprises the Central Nervous System (CNS), that is made up by the brain and the spinal cord, and the Peripheral Nervous System (PNS), that is made up by nerves that communicate with the other parts of the body. The PNS is then splitted in the afferent and efferent divisions. The efferent nervous system is further divided into the Somatic Nervous System (SoNS) and the Autonomic Nervous System (ANS). The first is responsible to innervate the skeletal muscles that control body movements. The ANS controls, largely in an unconscious way, bodily functions such as body temperature, blood pressure, heart rate variability, sweat glands activity, respiratory rate or pupillary response. Thus, the ANS innervates smooth muscle, cardiac muscle and glands to maintain the homeostasis and to respond rapidly to external stimuli. This predisposition to react is modulated by both branches of the ANS, the Sympathetic Nervous System (SNS) and the Parasympathetic Nervous System (PSNS). All these different systems have distinct functions, but all are interrelated and contribute to the proper functioning of the body [28, 37].

The biosignals studied in this work are from organs that are innervated by the ANS. Both ANS branches function in such a way as to exert opposing effects on the organs. The SNS is predominant in situations of arousal or stress where it increases the activity of the organs and the PSNS dominates in situations where the body is relaxing or needs to conserve resources. For example, sympathetic activity is responsible for the increase of Heart Rate (HR) and for the pupil dilation, while parasympathetic activity acts decreasing HR and contracting the pupil [21, 28, 29, 37].

Several studies have been conducted in order to identify the brain regions associated with decision making.

The dorsolateral and ventromedial subregions of the pre-frontal cortex are connected to the decision making behaviour in primates. The Dorsolateral Prefrontal Cortex (DLPFC)

encodes the evaluation of the response according to the state of the environment. The Ventromedial Prefrontal Cortex (VMPFC) is activated during decisions made in an uncertain situation [35, 71]. The Orbitofrontal Cortex (OFC) is linked to adaptive capacity when a previously correct decision ceases to be [41]. The Anterior Cingulate Cortex (ACC) enables the individual to adapt its decisions according to the outcome of its previous action, for example after making a mistake [40, 71]. The *parietal cortex* is thought to be involved in the evaluation of gain or loss magnitude, for example when decisions are made under risk situations [71].

Other regions, such as the *amygdala*, are also involved in decision making, so that a complex neural network is involved in the decision-making process. Through the research already done it is possible to conclude that different regions are implicated in different decision making behaviours, although the regions and their function are highly interrelated [71].

The regions in the frontal and the anterior cingulate cortex, involved in the decision making process, are represented in Figure 1.1.

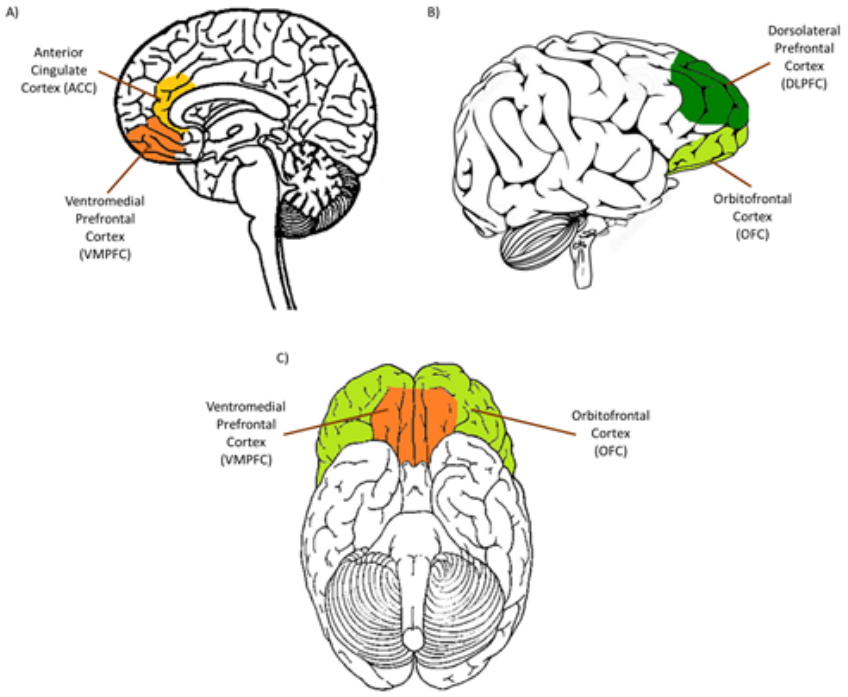

Figure 1.1: Brain regions involved in decision making. Yellow represents the ACC, orange the VMPFC, green the OFC and dark green the DLPFC. Different views of the brain are represented: A) Sagittal slice; B) Side view; C) Bottom view.

1.2.2 Biosignals

Every biological event, such as a beating heart, gives rise to physiological changes that can be measured, analysed and processed - the called biosignals. The record of these biosignals can be used to comprehend and explain a variety of physiological mechanisms. Through the diversity of these mechanisms, it is possible to conclude that the number of existing biosignals will be very high [68].

Biosignals can be classified based on their physiological origin [16], so there are:

- Bioelectric signals - measure of the electric field that is propagated by the cells, for example the ECG;
- Biomagnetic signals - measure of the magnetic fields, for example the Magnetoencephalogram (MEG) is used to obtain additional information about brain cells that the Electroencephalogram (EEG) can not give;
- Biochemical signals - give information about the levels of chemical substances in the body, for example the partial pressure of O_2 in our blood;
- Biomechanical signals - measure of mechanical functions such as motion, force or pressure, for example the mechanorespirogram detects changes in the diameter of the chest and gives information about respiration;
- Bioacoustic signals - measure of biological events that produce sounds, for example listening to the heart can help to diagnose heart valve's malfunctions;
- Other signals.

In this work, we will measure and process ECG, EDA, BVP and pupillometry.

1.2.2.1 Electrocardiogram

The ECG measures the electric activity of the heart. This activity is coordinated by a group of specialized heart cells that generate and conduct an electrical signal that maintains the heart beating in the right way. Thus, the ECG allows the evaluation of depolarization and repolarization of these cells that coordinate the mechanical pumping of the blood. This mechanical pumping is made of two important phases: the diastole, where the heart rests and its chambers fill with blood, and the systole, where the heart pumps the blood. These series of events between each pump are called cardiac cycle and can be distinguished in the ECG [5]. The ECG measurement is made using three electrodes usually laced on the chest, one serving as ground and the other two recording the electric activity of the cardiac muscle.

An example of a cardiac cycle shown by the ECG signal is presented in Figure 1.2. It is composed by a sequence of waves (positive and negative) with inter-wave segments

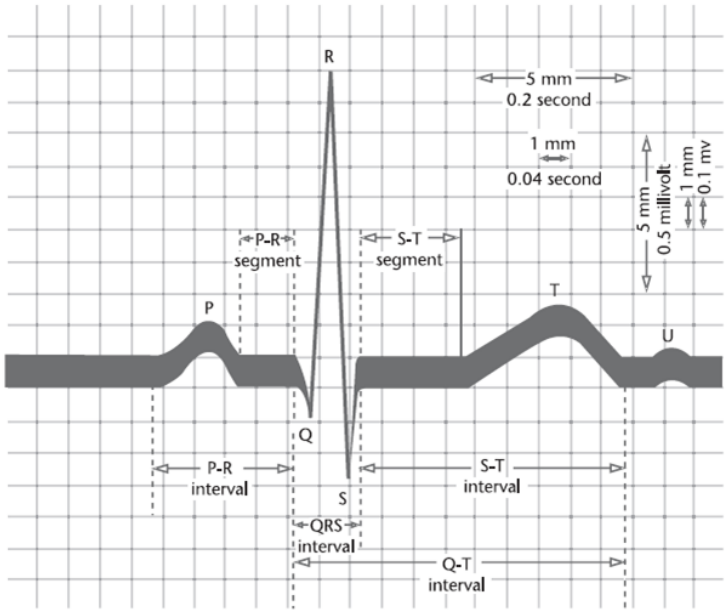

Figure 1.2: ECG signal with one cardiac cycle showing the P, Q, R, S, T and U waves and the segments between waves, from [34].

Table 1.1: ECG features, corresponding cardiac cycle's phase and duration time [37, 62].

ECG feature	**Cardiac cycle's phase**	**Duration time / ms**
P wave	Depolarization of the atrial chambers	< 110
PR interval	Atrial systole	120-200
QRS complex	Depolarization of the ventricular chambers	< 120
T wave	Repolarization of the ventricular chambers	100
QT interval	Ventricular systole and beginning of diastole	250–500

which depend of the propagation direction of the signal. In Table 1.1 is presented the meaning of the most important features of the ECG signal and its duration time.

Thus, the importance of the ECG lies in the fact that anomalies can be detected, such as the absence of the P wave or a QRS complex that is wider than normal, which allow the diagnosis of various pathologies [37]. Factors such as the decision-making process or the personality can also have an impact on HR. Crone and colleagues measured HR (and EDA) from subjects playing the IGT. Good performers HR decreased prior to a disadvantageous choice in relation to an advantageous choice. All participants experienced HR decreasing after a loss [26]. There are also studies that connect Heart Rate Variability (HRV) parameters with FFM personality traits [84].

The duration of each part of the cycle is influenced by the interaction between the SNS and the PSNS. The variation of the time between heartbeats (RR interval) is of particular interest - HRV [37].

The HRV reflects the change in cardiac activity since the HR changes quickly responding to the situation in which the person is. For example in a stressful situation, the SNS is stimulated causing an increase of the number of heartbeats. The PSNS, for example, in a trauma situation decreases the HR [12, 29]. In Figure 1.3 is shown an example of the HRV signal.

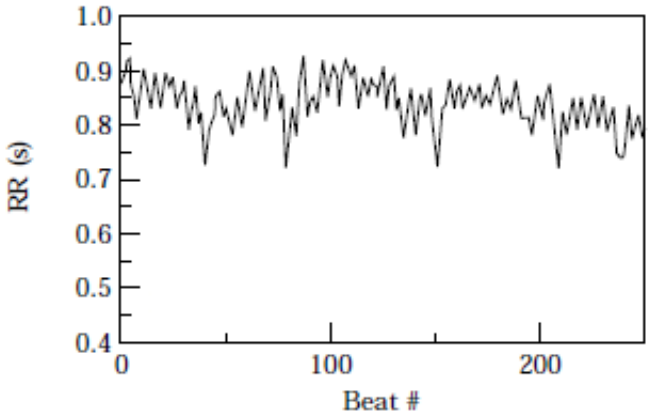

Figure 1.3: HRV signal, adapted from [12].

From the HRV signal, it is possible to extract linear (statistical, geometrical and frequency domain) and non linear features that are proven psychophysiological measures. The Standard Deviation of the NN interval (beat to beat interval) (SDNN), the HRV triangular index and the Ratio between Low and High Frequencies (LF/HF), are frequently used [12, 19, 29].

1.2.2.2 Electrodermal Activity

The skin is the largest organ of the human body and performs a wide variety of functions. It is composed by a large number of sweat glands that are densely innervated by the SNS. Through the glands secretion, changes in skin conductance can be measured after the application of a small current - this biosignal is called EDA. This measurement is made through a pair of electrodes that are positioned in the hands or feet. Since the applied current is constant throughout the measurement, it is possible to measure the electric potential difference between the electrodes and with this calculate skin resistance. The skin conductance is the inverse of the skin resistance [37].

As the sweat glands are directly related to the SNS, EDA is an extremely useful measure in the field of psychology because it allows a measurement of the physiological response to a stimulus [21, 54]. This conclusion was reached in several studies [3, 10], in which the number of active sweat glands, which are correlated to the electrodermal events, are related to SNS activation.

EDA measures the changes in tonic Skin Conductance Level (SCL) and the faster changes which are called Skin Conductance Responses (SCR). The latter one is associated with an increase in sweating that is measured through the current that flows between

two electrodes. These responses could be directly related to stimuli, Event Related Skin Conductance Responses (ER-SCR), or Non-Specific Skin Conductance Responses (NS-SCR) that are present without the registration of external stimuli [59]. Both SCL and SCR can vary from person to person.

In Figure 1.4a is represented an example of an EDA signal and in Figure 1.4b is showed the morphology of a SCR.

The maximum amplitude of the SCR is the most extracted feature in EDA, specially in psychophysiology, since it is considered an index of sympathetic activity [50, 54]. In the Table 1.2, the typical values of some EDA parameters are presented.

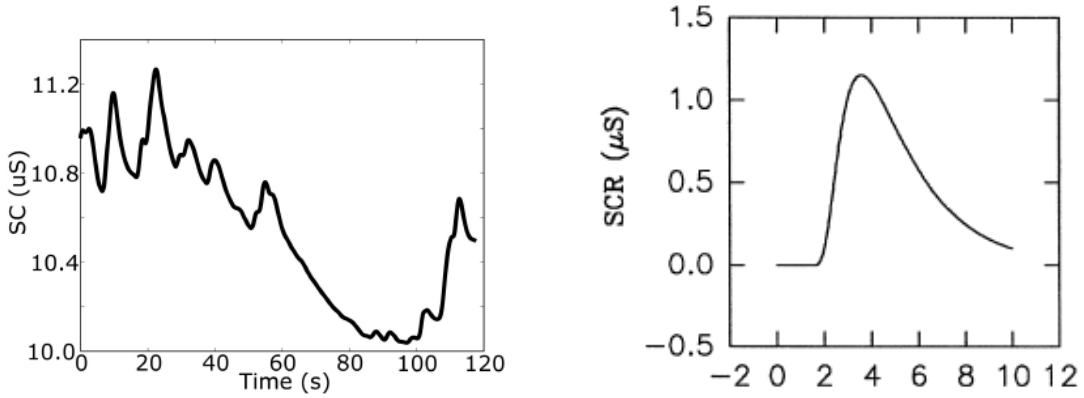

(a) (b)

Figure 1.4: (a) Example of an EDA signal, extracted from [38]; (b) Morphology of a SCR, extracted from [13].

Table 1.2: EDA features and respective definitions and typical ranges [37].

EDA feature	**Definition**	**Typical range**
SCL	Skin conductance level	2-20 μS
SCR latency	Time interval between stimuli and SCR beginning	1–3 s
SCR amplitude	Maximum amplitude of the SCR	0.1-1 μS
SCR rise time	Time interval taken to reach the peak	1–3 s
SCR half recovery time	Time interval between the SCR peak and the point where SCR amplitude reaches half its peak height	2-10 s

1.2.2.3 Blood Volume Pulse

The BVP measures the blood flow that passes through the tissues. In every heartbeat, a certain volume of blood is pushed through the body's arteries reaching its extremities and then returns to the heart through the veins. To measure this signal a Photoplethysmographic (PPG) sensor is used: this sensor emits an infra-red light that can be transmitted, absorbed or reflected by the tissue and it detects how much light returns to the sensor. This amount corresponds to the average of blood volume in the tissue where the light travelled [42, 63]. In Figure 1.5 is presented an example of a BVP waveform from one heartbeat.

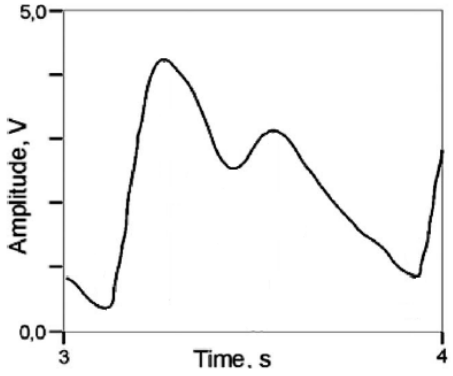

Figure 1.5: Example of a BVP waveform, adapted from [42].

The envelope of the BVP signal represents the relative constriction and dilation of the vessels and its directly correlated with the sympathetic activity of the ANS: in situations of fear or pain vasoconstriction occurs, as opposed to vasodilation that happens in relaxing states. HR (and HRV) can be extracted from the BVP since its signal reaches its peak in the ventricular systole, so the time between peaks corresponds to the time interval between heartbeats [42, 78]. More researchers are using this signal as a method to measure HRV since the PPG sensor is more comfortable to the user than the sensors used in medical settings to measure ECG. This signal is also useful on its own since the shape of the BVP wave is an indicative variable of cardiac health and its amplitude is correlated with the sympathetic and parasympathetic balance present in cognitive or emotional activity. For example, the BVP amplitude decreases in the presence of a stimuli that triggers the SNS or the BVP amplitude of a person more driven by their emotions takes longer to return to the their usual baseline level [42, 78, 94].

The usual features extracted from this signal are the SDNN, Root Mean Square of Successive period Differences (RMSSD), Number of pairs of successive NN intervals that differ by more than 50 ms (NN50) and other time and frequency domain features that are computed from the HRV signal, as well as features like the average amplitude and standard deviation of the BVP signal and the BVP peak-to-peak Amplitude Variation (BAV) [63, 78].

1.2.2.4 Pupillometry

Pupillometry is the study of the pupil diameter variation and its an research area that has been increasingly studied in the psychophysiological field since pupil dilation is a marker of ANS activity, more specifically of sympathetic activation [77]. The most important physiological function of the pupil is to adapt to the ambient light [45]. The pupil increases slowly its size after the occurence of a stimulus, approximately 1s, and, because of that, its acquisition is more common in tasks where events are separeted by a bigger time interval [72].

The process of pupil diameter acquisition is made using an eye-tracker device, which provides information not only about the pupil but also measures the point where the person is gazing. Nowadays the eye-tracker devices rely on a video-camera that tracks one or both eyes and records their moviment using the pupil.

In several studies [46, 52, 55], it is mentioned that the dilation of the pupil is connected with the decision making process, more specifically with the moments after the decision is made and consolidated. Due to this fact, the study of the pupil as a measure in the field of psychophysiological has been increasing. Pupil variation is also present during cognitive tasks processing [11, 47] and affective information processing [24].

In Figure 1.6 is represented the variation of the pupil diameter after the presentation of a visual stimuli.

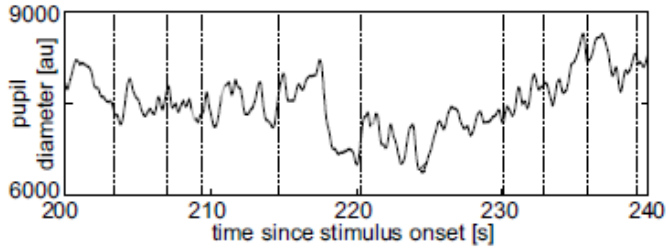

Figure 1.6: Pupil diameter variation, in arbitrary units, during the presentation of ambiguous visual stimulus, adapted from [46].

Common features extracted from this signal are the average pupil diameter, number of peaks and the Area Under the Curve (AUC) [24, 90].

1.2.2.5 Biosignal Monitoring

To monitor human activity, a balance between the number of sensors used to collect data and the acquisition of as much information as possible should be achieved, so that this monitoring does not become uncomfortable for patients or subjects from scientific studies [80]. The development of wireless sensors that can collect physiological data, with the same quality of the traditional devices, is an area of extreme interest in the field of Biomedical Engineering and that can provide more confort to patients, specially in cases where extensive periods of time are recorded.

The sensors used to acquire the biosignals have a series of pre-processing tools that allow more user-friendly results. Initially, the acquired analogical signal is amplified and filtered to remove background noise and other sources of interference. Then, the signal is discretized in amplitude and time so it can be digitally processed. In this step there is some loss of information but with advanced sensors this loss is minimized by a high sampling frequency (fs). This processing differs for each signal but common processing tools are filters and spectral estimators [30].

1.2.3 Human-Computer Interaction

Human–Computer Interaction (HCI) is a term that encompasses the influence of computer technology and its impact in human life. In the age we live in, this technology is present in almost everything from mobile phones, tablets, television, cars navigation systems and even in smart homes. So, HCI measures our interaction with these devises and allows the improvement of technology to make it more easy and appealing [51].

In this thesis, electrophysiological signals are extracted while the subjects are interacting with a computer programmed gambling task. The results of this interaction are utilized to predict personality.

1.2.4 Personality

In our daily lives, we have the constant need to classify people that surround us in an attempt to know how a certain person will react in a certain situation. That's why the term personality is used since Ancient history. There are various definitions given by different personality psychologists but all of them have a set of central ideas: personality can be described as an inner force that leads a person to act, to think or to feel in a certain, consistent way; it is not a set of different parts but, instead, an organization which gives us our singularity in relation to others; and it is not part of a specific organ, it is an active and dynamic process that occurs inside each individual [23].

Therefore, the aim of personality psychology is to find a theory that describes, explains and predicts human behaviour. To achieve this goal, there is an important distinction to be made, the difference between *personality traits* and *personality types* or *dimensions*.

The consistent, permanent way in which a person responds to different situations is called a *personality trait*. Common traits are impulsiveness, modesty, assertiveness or anxiety. The degree to which a person presents a particular trait is variable, so it can be said that these traits are dimensions of personal differences. All traits can be represented by a two-pole scale, in which the higher the score the greater the tendency of the individual to behave according to the trait in question. Consequently, the traits are found in all people but in a different degree, which has a normal distribution meaning that most people are in the middle of the scale and only a few are in the extremities. Lastly, traits are called sub-dimensions of personality [14, 23].

Thus, to a set of several traits corresponds a *personality dimension* or *personality type*. For example, according to Costa and McCrae [6], the dimension *Agreeableness* is linked to traits like trust, straightforwardness, altruism, compliance, modesty and tender-mindedness.

There are several personality theories and the greatest disagreement between them lies in the number of personality dimensions. In the 1980's and 1990's, personality psychology research expanded to different cultures, with assessment tools being adapted to different languages. Most researchers came to the conclusion that personality was divided into five basic dimensions, but the name of these dimensions was not always consensual. One of the theories that meets the most universal consensus is that of Costa and McCrae - the FFM - due to numerous validations [23].

The authors created several questionnaires, including versions for self-rating and hetero-evaluation or versions which measure each facet of every dimension, the Revised NEO Personality Inventory (NEO-PI-R), or evaluate the 5 basic dimensions, the NEO Five-Factor Inventory (NEO-FFI) (see Table 1.3) [7]. For the purpose of this thesis, the NEO-FFI questionnaire was chosen.

Table 1.3: Basic dimensions according to the FFM by Costa and McCrae, their meanings, facets and a list of adjectives attributed to people with high or low scores in them.

Dimensions	**Meanings**	**Facets**	**High Scores**	**Low Scores**
Neuroticism	Assesses adjustment versus instability; identifies individuals prone to disturbances	Anxiety; Hostility; Depression; Self-consciousness; Impulsiveness; Vulnerability	Depressed; Frustrated; Guilty; Low self-esteem; Insecure	Calm; Relaxed; Confident; Self-satisfied; Emotionally strong
Agreeableness	Involves human aspects of humanity	Trust; Straightforwardness; Altruism; Compliance; Modesty; Tender-mindedness	Unselfish; Caring; Emotionally supportive; Modest	Hostile; Indifferent to others; Self-centered; Jealous
Conscientiousness	Evaluates the organization, motivation and persistence to achieve objectives	Competence; Order; Dutifulness; Achievement striving; Self-discipline; Deliberation	Thorough; Neat; Well-organized; Ambitious	Disorganized; Undependable; Negligent; Lazy
Extraversion	Measures interpersonal interactions, activity level, need for stimulation	Warmth; Gregariousness; Assertiveness; Activity; Excitement seeking; Positive emotions	Dominant; Talkative; Sociable; Warm	Quiet; Reserved; Shy; Indifferent
Openness to Experience	Assesses the appreciation of new experiences; exploration of what is not familiar	Fantasy; Aesthetics; Feelings; Actions; Ideas; Values	Imaginative; Curious; Original artistic; Non traditional	Conservative values; Practical; Limited interests; Non artistic

1.2.5 Decision Making

Decision making plays a central role in our daily lives. It can be as simple as deciding to act or not to act or can involve much more difficult decisions with an array of different outcomes depending on the way which we choose to behave.

According to Balleine [35], decision making "refers to the ability of humans and other animals to choose between competing courses of action based on their relative value of consequences". So, in order to assess the decision making behaviour, the most common tasks involve choosing between several options. These tasks also help to study the influence of factors such as personality and stress on decision making. Stress has a well known influence at every stage of the decision-making process [71, 86], unlike personality which has not yet been studied profusely.

Thus, decision making is a complex and dynamic process that includes multiple steps that are interrelated with each other (Figure 1.7). The decision making process starts with the recognition of a problem, followed by the search of information for alternative ways of action. After this the different alternatives are evaluated to make the choice and the selected action course is implemented [86].

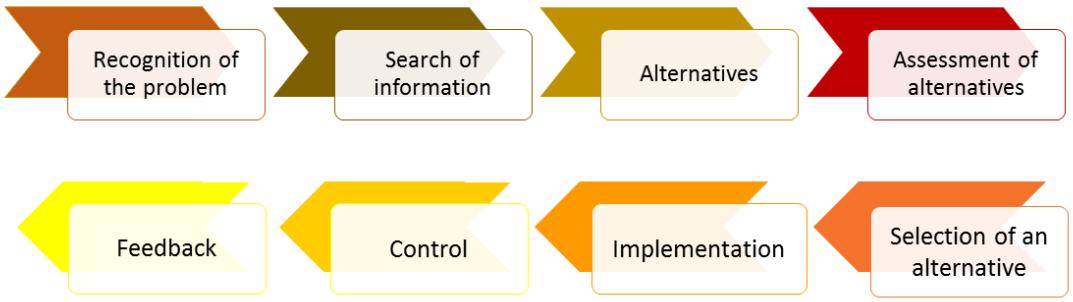

Figure 1.7: Steps of the decision making process.

Decisions can be categorized depending on the degree of uncertainty associated to them [71]. On decisions made under uncertainty the outcomes are known but their probabilities do not and on decisions made under risk the probabilities of the outcomes are known.

1.2.5.1 Maximization Theory

Several researchers, mainly in the second part of the 20th century, have proven that the theory that humans are rational choosers is wrong. According to Simon [1], the goal of maximization is almost impossible to achieve given the human cognitive limitations. So he proposed that in the face of a decision-making situation people tend to "satisfice". *Satisficers* evaluate their options until one of them is good enough. *Maximizers* search until the best option is found [22].

Since then, this theory has been studied by many. Schwartz gained prominence in his research that relates maximizer's behaviour and happiness. He argued that a bigger number of options to choose from is worse for maximizers, because more alternatives to examine causes more uncertainty in relation to the made decision. To satisficers more options may not have impact in their choice because their decision is already good enough. Through his research, he concluded that maximizers experience more regret, are more prone to be depressed and present a higher perfectionism index. On the contrary, satisficers are happier and more optimistic and have a higher self-esteem and higher life-satisfaction level [17, 22].

Thus, Schwartz developed questionnaires to measure regret and maximization behaviour, the *Maximization* and *Regret Scales* questionnaires [22]. These questionnaires were used in this thesis.

1.3 Objectives

The main objectives of this work are:

- Acquire and process biosignals (ECG, BVP, EDA, and pupillometry) during the realization of a human-computer interaction task;
- Implement a novel EDA processing method;
- Extract features from the biosignals;
- Find a correlation between events occuring on the IGT and events on the EDA signal;
- Predict specific personality traits, assessed through a HCI survey, through models constructed from the extracted features from all biosignals.

A schematic representation of this thesis work is presented in Figure 1.8.

Thus, this work started by looking for participants who fulfilled the necessary requirements for the objectives of this work. Their biosignals were recorded during the performance of IGT and after personality baseline data was gathered through the applied personality and decision making behavior questionnaires.

Other aim of this work is to implement and validate a novel mathematical model for the processing of the EDA signal that is based on a morphological analysis of the signal and that is able to detect and quantify single isolated events and overlapping and small amplitude events. After this, the objective was to develop a feature that is based on the SCR component of the EDA signal but that takes also into account the synchronization with IGT.

After the processing and feature extraction from all the signals, a prediction of personality was made, using machine learning algorithms, based on the subjects biosignals recorded during a task that simulates real-life decision making under situations of uncertainty. This prediction was made using each biosignal individually and to finish with the features from all the signals.

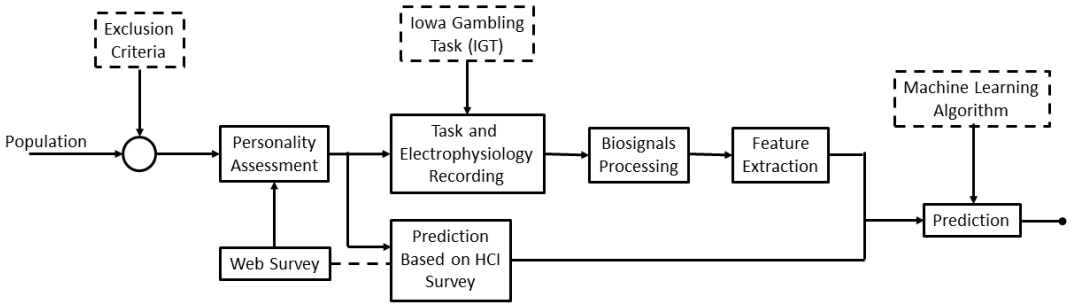

Figure 1.8: Schematic representation of the developed work.

1.4 Thesis Overview

The thesis basis is described in the chapter 1 and 2. In the first chapter is given an introduction to the motivation and contextualization of this thesis development, as well as a section with theoretical concepts that explain and describe topics that are essential to the comprehension of this project. The main objectives are covered in this chapter as well. Chapter 2 gives information about the state of the art in the areas covered by this thesis.

The experiment and the methodologies used to apply it are described in the chapters 3 and 4. Chapter 3 describes the experiment, as well as the population that takes part of the study and the conditions in which the data was collected. Chapter 4 describes the software and hardware material used throughout this thesis, as well as the methods applied to process the biosignals and extract features from them. The machine learning algorithm used for feature selection and classification is also explained in detail.

In the chapter 5 the results of the prediction models for each biosignal and for the combination of the four studied in this thesis are presented and discussed. The final chapter presents the conclusions of the work that was done and introduces some topics of future work to continue this study.

Chapter 2

State of the Art

2.1 Biosignal Monitoring

The development of equipments to measure biosignals is an area of extensive research in the biomedical engineering field. The conventional devices for physiological signals (PS) monitoring, still used in most hospitals, rely on infrared technology and rigid multi-electrode pressure sensors that limit their portability and wearability [82]. The recent technological development in miniature biosensing devices, smart textiles, microelectronics and wireless communications associated with the need to monitor PS out of the hospital environment has led to the development of wearable sensor-based systems with small sensors that can monitor PS at any time or place [58].

The PS monitors used in this work are the *Biosignalsplux* and the *SensoMotoric Instruments (SMI)*. The Biosignalsplux is a wearable, wireless device that provides a much comfortable method to record biosignals such as EEG, ECG or BVP, for extensive periods of time [95]. The SMI company provides eye tracking solutions such as mobile Eye Tracking Glasses (ETG) and Remote Eye tracking Devices (RED). Their technology, through video-camera, tracks the pupils and computes the gazing direction, the eyes movements and also points of regard, using sampling frequencies ranging from 30 Hz to kHz [96].

2.2 Personality Assessment

Due to its universal acceptance, the FFM questionnaires have been translated and validated to several languages. The NEO-FFI, a short version of the NEO-PI-R, has 60 items and measures the five basic dimensions. Its original version, written in USA English language by McCrae and Costa, has a *Cronbach's alpha*, used to measure internal consistency, that ranges from 0.68 to 0.86 [81]. A more recent version from the same authors has

been validated with better results, 0.75 to 0.82 [27]. The German-language version of the NEO-FFI, developed by Borkenau and Ostendorf [8], was validated and presented values of *Cronbach's alpha* ranging from 0.71 to 0.85 [20].

There are research being done that correlates personality traits with HRV. Results show a high negative correlation between Neuroticism and Power in High Frequencies (HF) and a high positive correlation with LF/HF. A negative correlation between HF and Openness to Experience was also noted [84].

Liza and colleagues (2016) analysed the influence of personality dimensions in concealing guilt. They were asked to commit a mock theft and after were tested in the Guilty Actions polygraph Test. Individuals with a low score on the Extraversion dimension showed larger SCR [87].

ASCERTAIN is a database that correlates the FFM personality scales to emotional states [88]. This relationship is measured through EEG, ECG, EDA and facial activity data features, linear and non-linear. These data is collected during affective movie clips visualization. The conducted analysis in this study suggests that non-linear statistics explain better the relation between emotion and personality dimensions.

In 2017, researchers collected and gathered in a database, AMIGOS, research on affect, social context, personality and mood of individuals and groups of four people. The physiological data, EEG, ECG and EDA, is recorded during the visualization of short and long videos and is used to correlate affective responses to personality and mood. The EDA features recorded during the long videos were the best predictors of personality traits, PANAS (self-report questionnaire that measures positive and negative affect) and social context, while EEG was the best predictor of valence and arousal affective states [92].

There are not many studies that directly correlate FFM personality dimensions with biosignals, specially with the combination of ECG, EDA, BVP and pupil diameter signals, so the work that will be done in this thesis can further develop this field.

2.3 Assessment of Decision Making Behaviour

Through the years several gambling tasks were developed in order to evaluate decision making behaviour. Most of them, like the IGT [9] or the Cambridge Gambling Task [15] were used to simulate decision making situations with a degree of uncertainty or risk.

The IGT was developed by Bechara and colleagues in 1994 [9]. This task is a card game that simulates decision making in a environment where the person receives feedback to evaluate the probability of gaining a reward or getting punished. With the feedback of the money lost or won, given after each round, the player should conclude that the card decks associated with a high gain are associated with a high loss and the card decks with low gain are associated with a low loss, so the latter are more advantageous in the long run [9, 75].

Performance on IGT can be measured through the difference between the total sum of choices of advantageous decks minus the total sum of choices of disadvantageous decks

or the number of cards chosen from the advantageous and disadvantageous decks during the five consecutive blocks of the task, which allows the tracking of the learning evolution of the players [31, 36, 75].

The performance in the IGT can be correlated with the level of maximization of the person. The original versions of the Maximization and Regret Scales, developed by Schwartz et al. [22], have an *Cronbach's alpha* value of 0.71 and 0.67, respectively. The German-language version [32], used in this study, also had good results of internal consistency with a *Cronbach's alpha* of 0.67 and 0.77 for the Maximization and Regret Scales.

Goudriaan and colleagues (2006) conducted an experiment where they compared the performance on the IGT of a pathological gamblers (PG) group with a normal control (NC) group while recording ECG and EDA. The PG group showed lower SCR and a decrease in HR while they were pondering about what to choose. After both loosing and winning the PG presented a decrease in HR, while the NC group presented an increase after winning and a decrease after loosing [31].

Claudio Lavín and colleagues (2014) studied pupil dilation during the performance of IGT. Their results showed that the pupil diameter increased during the presentation of positive feedback, when in a learned uncertain situation, and in the negative feedback presentation as weel, influenced by surprise [79].

In 2017, HRV and EDA signals were monitored during the IGT, and other gambling tasks, in order to measure the influence of anxiety and depression in decision making behaviour. The results showed that anxiety and sympathetic reaction to losses are strong predictors of good scores in the task. Depressed participants with low tonic HRV predict worse IGT performance [93].

There is little research that correlates biosignals acquired during the performance of HRV with the FFM personality traits. In that way, this work can help unveil the impact of personality in the performance of IGT and consequently, in the decision making process.

Chapter 3

Methods

In this chapter are described the methologies used throughout the development of this thesis. First there is a description of the used software and hardware materials; then it is given an explanation about the personality assessment questionnaires and the last sections present the computational methods used for the biosignals processing, the extraction of features and the machine learning algorithm developed to find the best combination of features to predict the FFM and Maximization and Regret scales.

3.1 Technological Materials

The *LimeSurvey* web application was used to conduct the web surveys and the collected data was extracted through a *csv* file to be processed later.

To acquire the ECG, EDA and BVP signals, the *Biosignalsplux*, a wearable device with 8 analogue channels and bluetooth connection, was used [95]. This device has the following sensors:

- Electromyography;
- **Electrodermal activity**;
- **Electrocardiogram**;
- Electroencephalogram;
- Accelerometer;
- Temperature;
- Respiration;

- Force;
- Light;
- Foot switch;
- Pushbutton;
- Goniometer;
- Load Cell;
- Vaginal Electromyography;
- RFID Sensor;
- SpO_2 Sensor;
- **Blood volume pulse**;
- Force platform.

The *SMI RED* [96] was used to acquire the eye-tracking data.

The IGT was programmed in the *Presentation* software from Neurobehavioral Systems [98].

Data acquisition was conducted using in-house done software based on Python language. This software connects and synchronizes the *Biosignalsplux* device, the eye tracker and the IGT program and returns a file with all the acquired data.

To process these biosignals, the code editor PyCharm v2016.3.3 was utilized using Python v3.6.0 language [64, 101]. The Python Packages used for data visualization were Matplotlib v2.0.0 [39] and Seaborn v0.7.1 [99]. NumPy v1.11.3 [66] is the standard package used for numerical computation in Python. SciPy v0.19.0 [73] supplies advanced mathematical functions, such as integration and statistical functions, supported by NumPy arrays. Pandas v0.19.2 [56] provides data structures and statistic tools used to compute large data sets. Scikit-learn v0.18.1 [65] is a Python package with a variety of implemented state-of-the-art machine learning algorithms for supervised and unsupervised problems.

The package *novainstrumentation* [97], used on Digital Instrumentation class at Faculdade de Ciências e Tecnologia, Universidade Nova de Lisboa, was also used in the processing of ECG, specifically in the QRS complex detection. The *PyEEG* v0.02 r2 module is a open source tool focused on the extraction of non-linear features from the EEG signal, such as the Approximate Entropy (ApEn) or the Hurst Exponent (Hurst), that in this thesis were applied to the extraction of non-linear features from the HRV signals [60]. The nolds v0.2.0 module provides tools for the extraction of nonlinear parameters from one-dimensional time series [100].

3.2 Biosignals Processing

In this section, the algorithms applied to process each biosignal are described. The processing of all signals was made after its acquisition. All the processing tools used in this work come from the Python packages mentioned in the section 3.1. Subjects whom synchronization between physiological data and IGT times was not possible were discarded. All biosignals were segmented to exclude the data that was acquired before and after the task ended, so that only the data collected during the IGT could be analyzed. Also, ECG and EDA data were converted from Analog-to-Digital Converter (ADC) to mV and μS, respectively, and the pupillometry data from pixels to mm. The BVP signal does not have a standard unit.

3.2.1 Electrocardiogram

In the fluxogram presented in Figure 3.1 are shown the steps followed for the processing of ECG.

First the signal is normalized and filtered with a Butterworth bandpass filter of 8 - 30 Hz. These cut-off frequencies were chosen in order to extract only the frequencies of interest of the R wave [18] (see Figure 1.2) since the next step of processing involves peak detection. The purpose of this filter is also to remove high frequency noise, baseline wandering and the respiratory rate component, which is generally inferior to 0.5 Hz.

The peak detection was performed using an implementation of the Pan-Tompkins algorithm [4], from *novainstrumentation* refered in the section 3.1. This algorithm reliably detects the QRS complex of the ECG signal, allowing the extraction of HR and HRV which are final results of the ECG processing that are used for feature extraction.

The next step consists on outlier detection. To do this the RR interval was analysed. If this interval was between 0.4 and 2 s or between 30 and 150 beats per minute (bpm), its value was replaced by the last value of RR interval. This range was chosen since the normal HR for a healthy person is between 60 and 100 bpm, however in certain situations the HR can be increased or decreased by ANS activity so a larger interval was used in this study. If the outliers percentage exceeded 5%, the subject was discarded from the study. For all other subjects HR, HRV and the HRV histogram and the HRV Power Spectrum Density (PSD) estimation were computed as final results of the ECG processing.

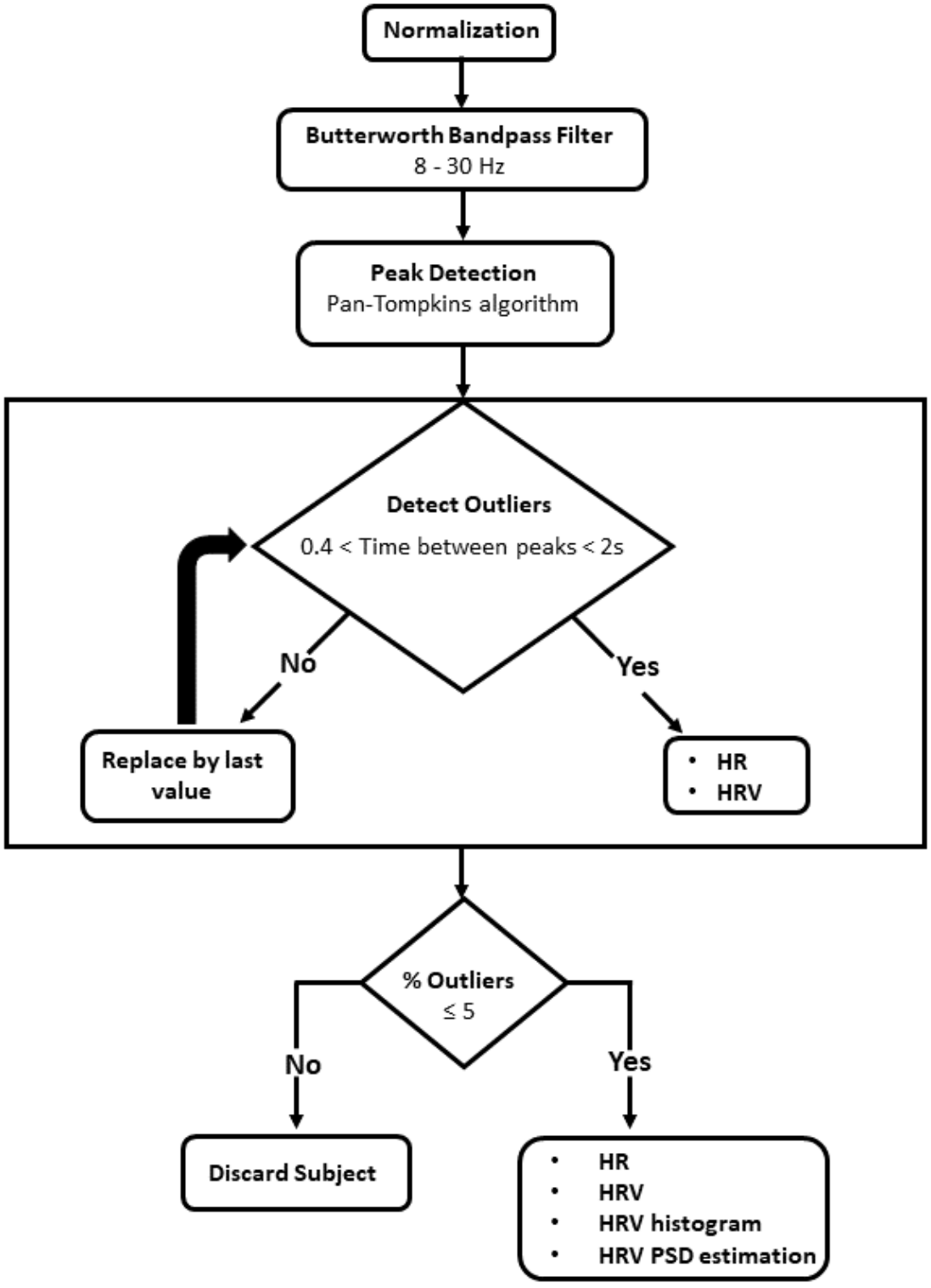

Figure 3.1: Processing tools for ECG and final outputs.

3.2.2 Electrodermal Activity

In Figure 3.3, the processing steps used to extract the SCR and SCL are presented through a fluxogram.

Initially the EDA signal is filtered with a low-pass Butterworth filter with a cut-off frequency of 1 Hz and then, to decrease its complexity, it is down-sampled to 100 Hz since the frequencies of interest are within the range 0 to 1 Hz. The Nyquist theorem dictates that the fs must be at least two times superior to the maximum frequency of interest so that information contained on the signal is not lost [33]. Thus, according to Nyquist, this down-sample step does not cause loss of information since in this case, the fs must be at least 2 Hz.

Then, the psychophysiological EDA model described in [38] was implemented with the objective of testing its validity and efficiency when processing EDA recorded during the performance of a gambling task as well as its utility for the extraction of features used to predict personality. This mathematical model is focused on the morphological characteristics of the EDA signal and solves other models main issues - the detection of overlapping EDA events and the detection of low amplitude events. Some alterations were introduced in order to decrease the computation time, such as the suggested cut-off frequency of the low-pass filter which was 2 to 5 Hz.

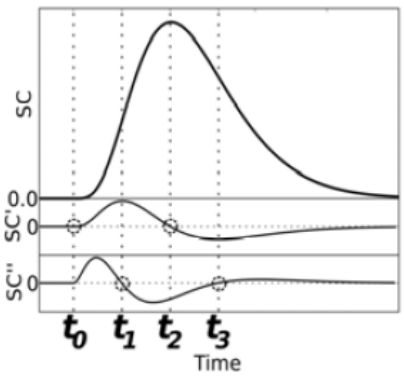

Figure 3.2: SCR morphology and respective first and second derivatives, from [38].

The first step of the algorithm, after filtering, is to compute each SCR. The morphology of the SCR is represented in Figure 3.2. To do this, the algorithm suggests the calculation of the second derivative zeros to extract the time parameters (t_1 and t_3), needed to reconstruct each SCR. Instead of this, the calculation of the maxima and minima from the first derivative was executed since it proved itself more time efficient in terms of computation and it has the same mathematical meaning.

Then, a step to select the peaks was implemented to set aside smaller peaks that are not important for this study. The chosen criteria was to forgo the peaks in which the time difference between t_1 and t_3 was smaller than 0.4 s. The peaks that surpass the selection criterion are reconstructed by calculating the t_0, a and b parameters of each SCR. These

parameters are used to compute each peak through the formula present in equation 3.1, where u(t) represents the unitary step function.

$$h(t) = a(t - t_0)^4 e^{-b(t-t_0)} u(t - t_0) \tag{3.1}$$

t_0 parameter is related to the SCR onset and it is calculated through Equation 3.2. a is connected with the event amplitude and b with the decay time of the SCR after its peak. Their computations are made according to Equations 3.3 and 3.4.

$$t_0 = \frac{3t_1 - t_3}{2} \tag{3.2}$$

$$a = b^3 \frac{f_{t_1}^{'} - f_{t_3}^{'}}{16e^{-2} + 432e^{-6}} \tag{3.3}$$

$$b = \frac{4}{t_3 - t_1} \tag{3.4}$$

After this, the SCL is computed subtracting the sum of all SCR to the filtered EDA signal.

Lastly, the sum of SCL variation was used as criteria to discard the subjects whose data acquisition had problems due to misplacement or displacement of the electrodes. As final outputs of the EDA processing, the sum of SCR, the SCL and the filtered EDA were used for feature extraction.

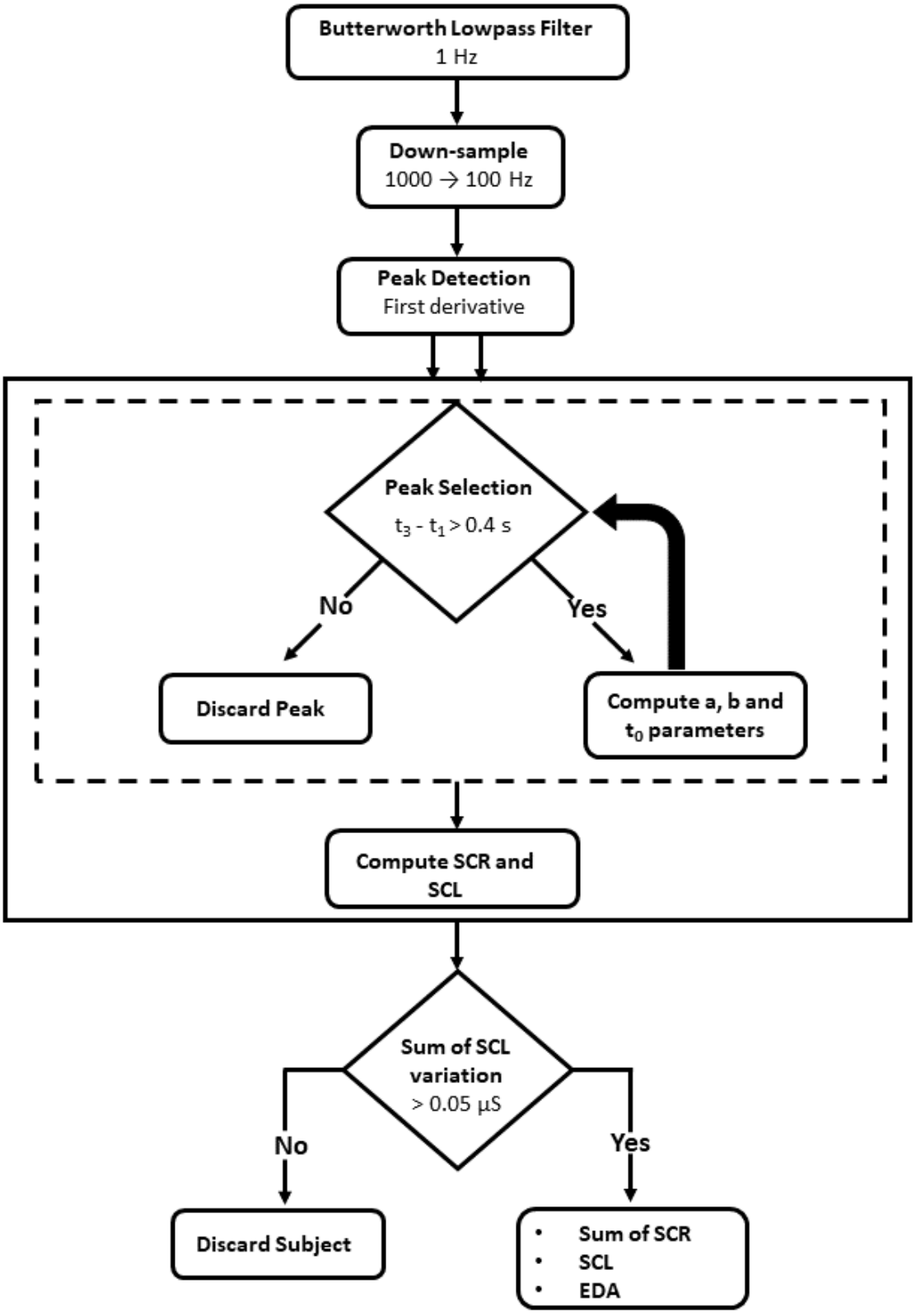

Figure 3.3: Processing tools for EDA and final outputs.

3.2.3 Blood Volume Pulse

In Figure 3.4, the fluxogram presents the steps followed to process the BVP signal.

The processing of the BVP signal starts by filtering it with a bandpass Butterworth filter with cut-off frequencies of 0.02 and 2 Hz. These filter is chosen since the bandwidth of the BVP sensor ranges from 0.02 to 2.1 Hz. After this, the signal is down-sampled to 250 Hz, which according to the Nyquist theorem does not cause any loss of information.

For the detection of the BVP peaks was implemented an algorithm adapted from [57]. This algorithm starts by computing the Slope Sum Function (SSF) of the BVP signal, present in equation 3.5 where w is the lenght of the time window and BVP_k the filtered BVP signal. The aim of this step is to enhance the onset of the BVP peak and to detect the SSF local maxima. The SSF peaks are selected using the adaptive threshold presented by Zong and colleagues in [25]. After this, a backsearch routine is performed in the cases where the time difference between successive peaks is bigger than 110%. With the detection of the SSF onsets and local maxima, the onset and maximum value of each BVP peak was computed.

$$ssf_i = \sum_{k=1-w}^{i} \triangle u_k, \triangle u_k = \begin{cases} \triangle BVP_k & : \quad \triangle BVP_k > 0 \\ 0 & : \quad \triangle BVP_k \leq 0 \end{cases} \tag{3.5}$$

The time interval between BVP peaks corresponds to the time between heartbeats, just like the time interval between QRS complexes of the ECG signal, so HR and HRV can be computed from BVP. People whose maximum time value between BVP peaks exceeded 2 s are discarded since this was the criteria also used for the ECG signal. The final outputs of the BVP processing are the filtered BVP signal, the BVP peaks onset and maximum.

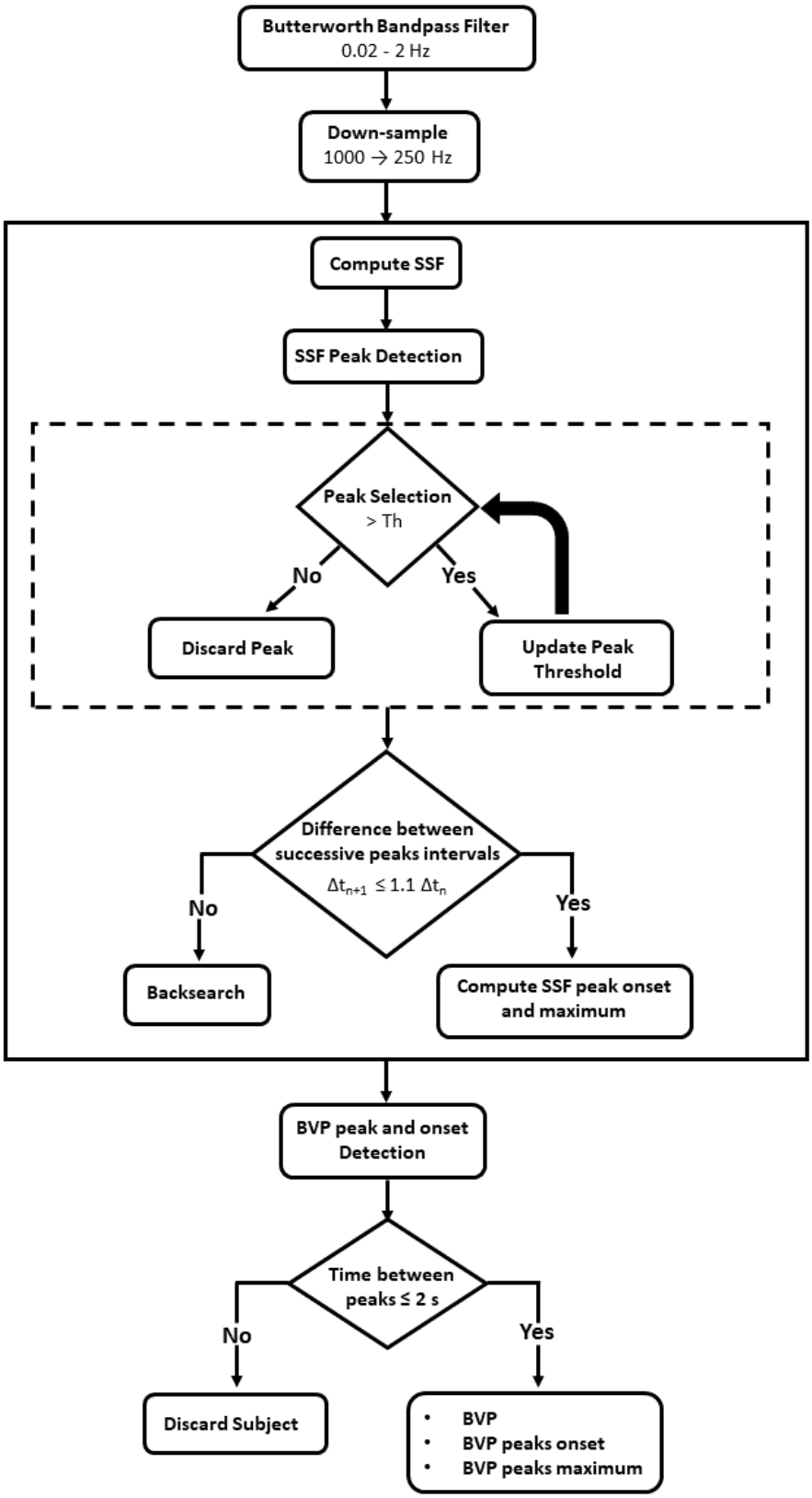

Figure 3.4: Processing tools for BVP and final outputs.

3.2.4 Pupillometry

In Figure 3.5, the processing steps used to extract information from the pupillometry data are presented through a fluxogram.

The first performed step to process the pupil diameter segmented the signal into three: data from the selection, choice and feedback phases of the IGT. The data from these segmentations was processed the same way. For the detection of peaks, the chosen criteria was the pupil dilation, if it was greater than 0.5 mm it was considered a peak in diameter.

Lastly, the percentage of time the subject was blinking or looking away from the screen was analysed. This moments corresponded to the zero values present in the pupil dimater data and were cutted from the signal. If this percentage was superior to 35% the subjects were discarded. As final outputs of the pupillometry data processing, the pupil diameter, the number of peaks and the blinking percentage were used for feature extraction.

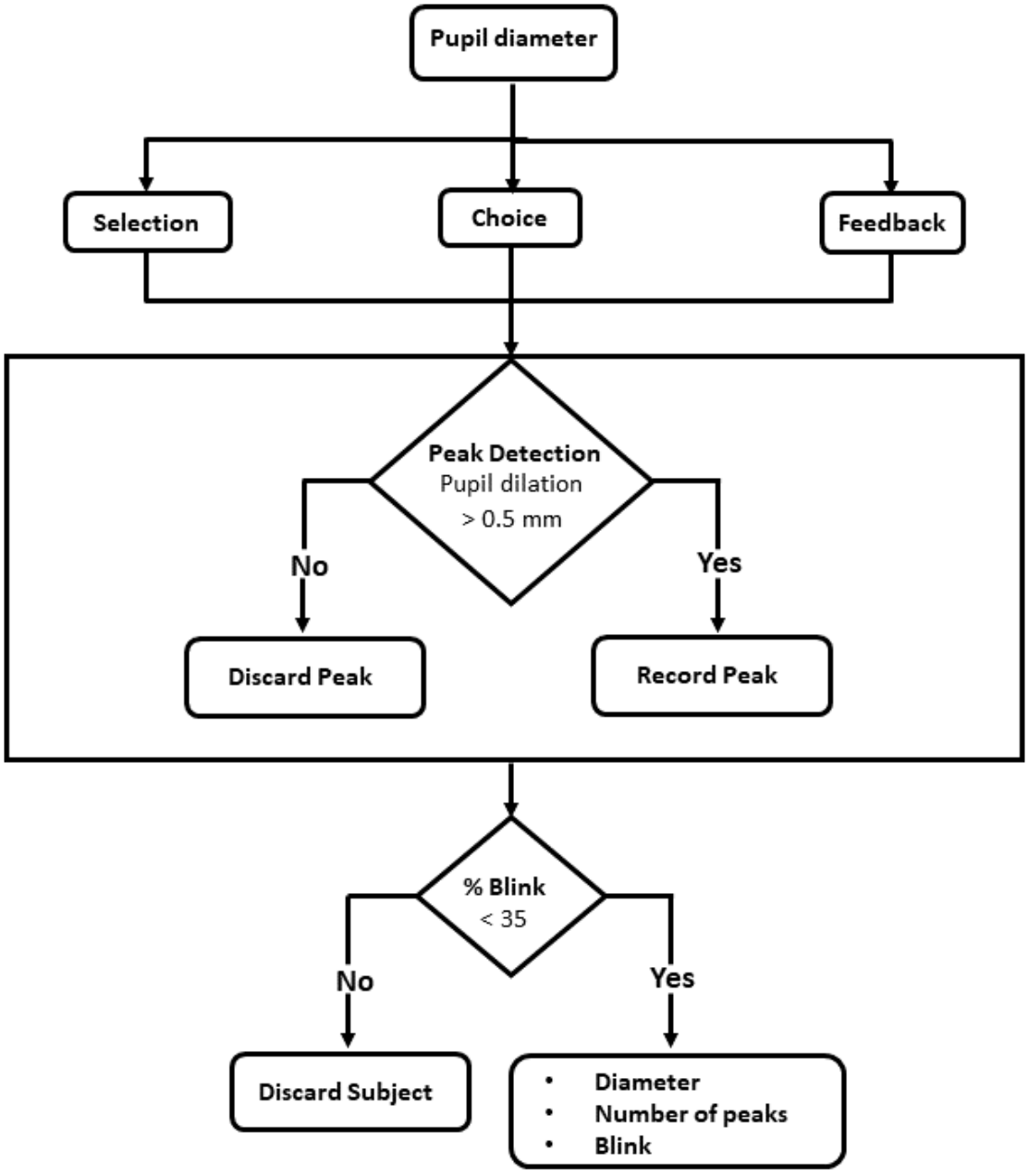

Figure 3.5: Processing tools for the pupillometry data and final outputs.

3.3 Features Calculation

The features computed from each signal are presented in this section. All features were extracted from the signal recorded during the complete performance of IGT and the same features were also extracted dividing the task in five blocks of 20 trials. In other studies [36, 61, 91], this division is made based on the fact that, in the first blocks, the players are still learning which of the decks are advantageous or disadvantageous and, in the latter ones, they already know which decks are the best for the long run.

3.3.1 ECG Features

In the Tables 3.1 and 3.2 are presented the features that were extracted from the HR and the HRV. Statistical features (mean, standard deviation, maximum and minimum) were computed from HR and HRV. Since HRV is a relevant tool to assess the sympathetic and parasympathetic functions, a series of linear and non linear features were extracted.

Most of the statistical, geometrical and frequency domain features are well known parameters that have been used in other psychological studies [43, 48, 85]. RMSSD, NN50 and the Percentage of NN differences greater than 50 ms (pNN50) are associated with short term, high frequency variations in HR while the SDNN (standard deviation of the HRV) and the HRV triangular index are estimators of the overall HRV [12].

The HRV triangular index, Triangular Interpolation of the NN intervals (TINN) and stress index are geometrical features that are computed from the HRV histogram - histogram presented in Figure 3.6a. The stress index is a measure of the level of activity prevalence of central mechanisms regulation above ANS. The logarithmic index, ϕ, is computed from the histogram of absolute differences between adjacent NN intervals where ϕ is the coefficient of the negative exponential curve that best approximates the histogram form [12]. Standard Deviation of instantaneous beat-to-beat variability (SD1), Long-term Standard Deviation of continuous NN intervals (SD2) and Ratio of short interval variation to long interval variation (SD1/SD2) are features extracted from the Poincaré plot of the HRV (Figure 3.6b).

For the computation of the frequency domain features, the PSD was estimated, according to the Welch method, in order to obtain the distribution of power in function of the frequencies that compose the HRV signal. Prior to this, the HRV signal was interpolated (cubic spline interpolation) due to it being an unevenly spaced signal and for the PSD estimation the signals must be evenly spaced in time. The interpolated HRV signal has a fs = 4 Hz. The most computed features are the Power in Low Frequencies (LF) and HF as well as the LF/HF. The LF component is in an indicator of sympathovagal balance, while the HF component is only related to the parasympathetic activity and the LF/HF measures the predominance of the sympathetic or parasympathetic systems [85].

More recently non linear features have also started being part of the research in this area [44] since they could provide more useful information on HRV. These features are

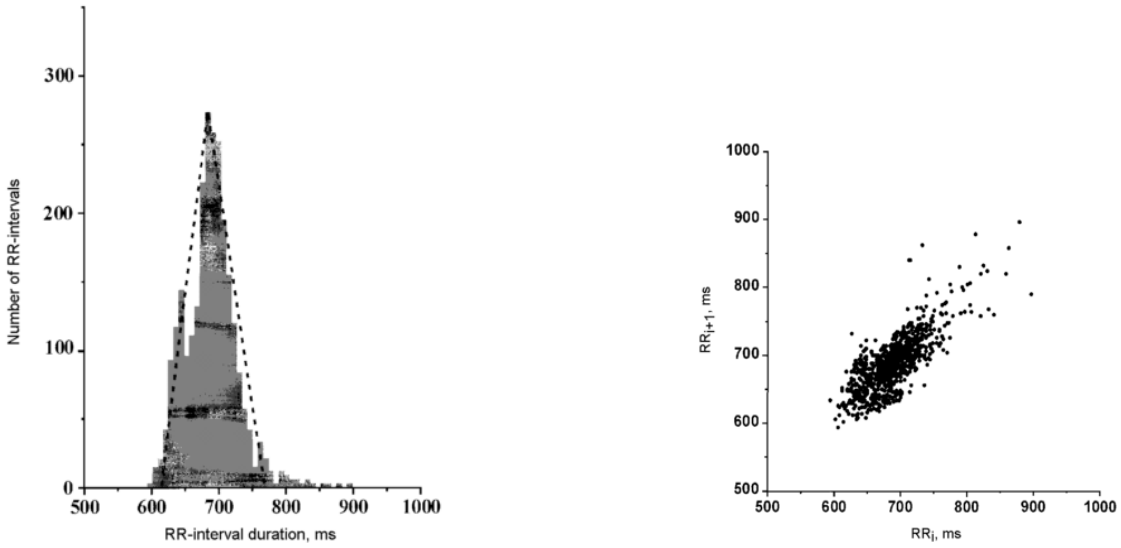

(a) (b)

Figure 3.6: Examples adapted from [19]: (a) HRV histogram with the triangular interpolation marked with black dashed lines to compute the TINN; (b) Poincaré plot.

based in chaos theory [29]. Correlation dimension (CD) measures the self-similarity of the signal with the Grassberger-Procaccia algorithm and its value increases in presence of chaotic data and decreases if HRV decreases as well [83]. ApEn measures the unpredictability of fluctuations in time-series, so a time-series with repetitive patterns scores low in this feature while a more complex signal has a high score; Largest Lyapunov Exponent (LLE) evaluates quantitatively the dependence on the initial conditions [44]. Sample Entropy (SampEn) evaluates complexity in a similar way to ApEn; the Fractal Dimension (FD) assesses the number of units that compose a curve in comparison with the minimum number of units that is required to reproduce a pattern of the same spatial size, according to the Higuchi algorithm; the Hurst measures the presence of long-term dependencies of the time-series and the degree of these dependencies; the α slope is a parameter extracted from the Detrended Fluctuation Analysis (DFA) of a signal that quantifies fractal scaling properties of NN intervals and it is an estimator of roughness of the time-series - the bigger the α the smoother the time-series [29]. The autocorrelation parameter was computed using a time lag of 5 heartbeats as suggested in [53].

Table 3.1: Statistical and geometrical features extracted from ECG signal. From the features marked with *, statistical parameters are computed. All other features are computed from HRV.

Feature	**Meaning**
Statistical	
HR*	Heart rate
HRV*	Heart rate variability
CV	Coefficient of variance
SDSD	Standard Deviation of Differences between adjacent NN intervals (interbeat intervals)
RMSSD	Root Mean Square of Successive Period Differences
NN50	Number of pairs of successive NN intervals that differ by more than 50 ms
pNN50	Proportion of NN50 divided by the total number of NN intervals
NN20	Number of pairs of successive NN intervals that differ by more than 20 ms
pNN20	Proportion of NN20 divided by the total number of NN intervals
Geometrical	
HRV triangular index	Integral of the density distribution divided by the maximum of the density distribution
TINN	Triangular Interpolation of NN interval histogram
SI	Stress index
ϕ	Logarithmic index
SD1	Standard deviation of instantaneous beat-to-beat variability
SD2	Long-term standard deviation of continuous NN intervals
SD1/SD2	Ratio of short interval variation to the long interval variation

Table 3.2: Frequency domain and non linear features extracted from ECG signal. All features are computed from HRV.

Feature	**Meaning**
Frequency domain	
VLF	Power in Very Low Frequencies (f < 0.04 Hz)
LF	Power in Low Frequencies (0.04 < f < 0.15 Hz)
HF	Power in High Frequencies (0.15 < f < 0.4 Hz)
LF/HF	Ratio between low and high frequencies
Total power	Total power (f < 0.4 Hz)
% VLF	Ratio between VLF power and total power
% LF	Ratio between LF power and total power
% HF	Ratio between HF power and total power
LF_{nu}	Relative value of LF power in proportion to the total power minus the VLF component
HF_{nu}	Relative value of HF power in proportion to the total power minus the VLF component
VLF peak	Frequency of the maximum value of the VLF
LF peak	Frequency of the maximum value of the LF
HF peak	Frequency of the maximum value of the HF
Non linear	
CD	Correlation Dimension
SampEn	Sample entropy
α slope of DFA	Fractal scaling
H	Hurst exponent
LLE	Largest Lyapunov exponent
FD	Fractal dimension
ApEn	Approximate entropy
Autocorrelation	Correlation of the time-series with a delayed form of itself

3.3.2 EDA Features

In Table 3.3 are presented the features computed from the processed EDA signal. The separation of NS-SCR and ER-SCR is not possible to achieve due to the complexity of the stimulus of this study, the IGT. Therefore there was no separation of SCR and the features extracted from SCR take into account both types.

The SCL and the NS-SCR frequency and mean amplitude are considered measures of general psychophysiological activation, specifically sympathetic activation [21, 74]. So, from the SCL were computed statistical features as well as from SCR amplitude and frequency (peak rate). Other features that often are extracted in other studies are the half recovery time and rise time [70, 76].

Table 3.3: Features extracted from EDA signal. From the features marked with *, statistical parameters are computed.

Feature	**Meaning**
SCL*	Tonic level of skin conductance
SCR	Number of detected peaks
Number of SCR in selection (%)	Ratio between the number of peaks in selection phase and the total number of peaks
Number of SCR in choice (%)	Ratio between the number of peaks in choice phase and the total number of peaks
Number of SCR in feedback (%)	Ratio between the number of peaks in feedback phase and the total number of peaks
SCR peak rate*	Number of peaks per minute
SCR amplitude*	Maximum height of the peaks
SCR rise time*	Time from the beginning until the maximum of the peak
SCR half recovery time*	Time to reach half the maximum value of the peak
Correlation with loss	Correlation between EDA based functions and the losses on the IGT

Due to the fact that the biosignals acquisition was made during the performance of IGT, features that take into account the synchronization of EDA events with the IGT events were computed. In Figure 3.7 an example EDA signal is presented with the peaks detected in selection phase marked with yellow dots, the ones in choice phase marked with orange dots and the ones in feedback phase marked with red dots. Thus, the number of peaks in each phase in relation to the total number of peaks detected are extracted as features.

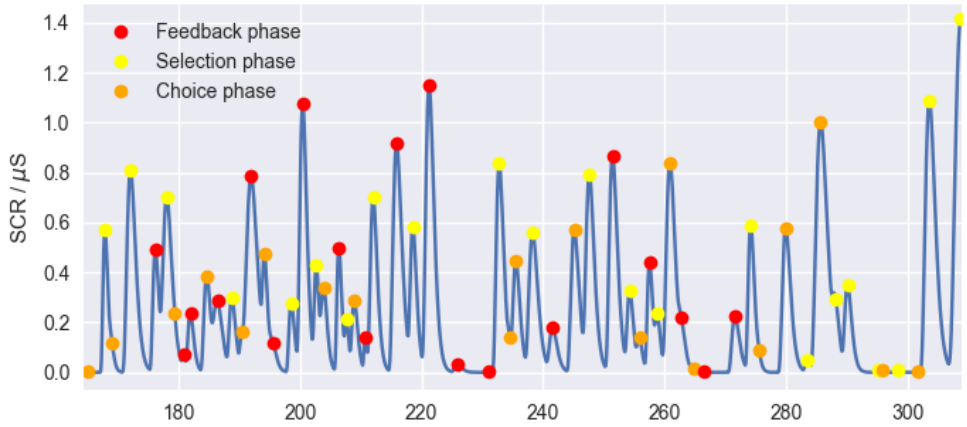

Figure 3.7: SCR component of the EDA signal. The detected peaks are marked according to the IGT phase in which they are detected.

In [89], it is reported that losses on IGT provoke a stronger physiological reaction in relation to equivalently sized wins. With that in mind, several EDA based functions were created with the objective of correlating these functions with losses on IGT. The first step was the creation of several EDA based functions proportional to the number of SCR as well as their height and area. The following functions were calculated for each instant of the IGT using a time window of equal size before and after each peak:

- Number of peaks;
- Average of the SCR component;
- Mean of peaks height;
- Sum of peaks height;
- Mean of squared area - the peak was approximated to a rectangular shape, with height equal to the peak height and width equal to the difference between the t_1 and t_3, and its area was calculated; after, the average value of the areas was calculated;
- Sum of squared area - the peaks were calculated using the same logic present in the previous function, but alternatively their areas were added;
- Mean of gaussian area - the peak was approximated to a gaussian curve, with height proportional to the peak height and width to the difference between the t_1 and t_3, and its area was calculated; after, the average value of the areas was calculated;
- Sum of gaussian area - the peaks were calculated using the same logic present in the previous function, but alternatively their areas were added.

To calculate the correlation between these functions and the losses on IGT, a time-series based on the losses on IGT was created. So, at the time of each loss on IGT, a gaussian curve is considered resulting in a waveform with the length of the EDA signal acquired during the IGT. Two gaussian curves were considered: one where the width of the gaussian is proportional to the loss, equation 3.6, and the other where the loss is proportional with the height of the gaussian, equation 3.7. t_{loss} corresponds to the time the loss occurs on IGT, t to each instant of the IGT, w to the chosen time window in seconds and $lost$ to the amount of lost money.

$$loss_{width} = e^{-\left(\frac{t_{loss}-t}{2*(0.001*w*(log(-lost))^2)}\right)^2} \tag{3.6}$$

$$loss_{height} = log(-lost) * e^{-\left(\frac{t_{loss}-t}{2*0.01*w}\right)^2} \tag{3.7}$$

The next step was to compute the correlation coefficient of each EDA function with the two loss waveforms. Prior to these correlations, the functions were segmented in five blocks and the correlations were performed to each block independently. It is also important to refer that for each person a different time window can be selected since the time window can assume a value between 1 and 30 s, so the time window which gave the best correlation was selected. In addition to this, the correlations were performed for different time shifts, with lags from -20 to 0 s, between the EDA based functions and the loss wave. This time shift is important since the reaction time of each person to the loss can be different. Concluding, for every EDA based function the correlation between itself and the loss wave is made for all time windows, between 1 and 30 s, and for all time shifts, between -20 and 0 s, and the highest correlation is recorded as well as the correspondent time window and time shift.

For example, subject 28 highest correlation between the 'Average of the SCR component' function and the $loss_{width}$ wave in the first IGT block is presented in Figure 3.8a. In the first plot, in vertical red lines are marked the moments when there are losses and in green the moments when there are wins on IGT. The wider the lines the bigger the loss (or win). In the second plot, it is represented the $loss_{width}$ wave composed by two added gaussians at the moments of loss that occur in the first block. As can be seen in the first plot, the second loss is much more significative than the first and, as a result, the second gaussian added to the loss wave has a larger width. In the third plot, it is represented the 'Average of the SCR component' function for the first IGT block. From the visualization of the second and third plots, it is evident that the correlation between them should be high. The correlation coefficient of these two waves is approximately 0.89 and the 'Average of the SCR component' function was calculated with a time window of 30 s and a time shift of -8 s.

After, the same computation was made but with the $loss_{height}$ wave. The results are shown in Figure 3.8b. For these results, it is visible that the correlation between the

'Average of the SCR component' function and the loss wave is not as high. The computed correlation coefficient is approximately 0.47 and the time window was 30 s and the time shift of -6 s.

When the losses on IGT are proportional to the width of the gaussians, the correlations are usually higher than the ones obtained for the loss proportional to the height of the gaussian. These results are verified for almost all subjects. Thus, all the correlations between the EDA functions and the $loss_{width}$ wave were chosen as features. The mean value of the correlations for the different EDA based functions was also used as a feature. This computation was independently made for the five blocks in which the IGT is divided.

(a)

(b)

Figure 3.8: The first plot of each subfigure has marked in red the moments where the subject loses money and in green the moments where he wins. The second and third plots are the loss wave and the EDA based function 'Average of the SCR component' for the 1st block. In (a) are presented the results for the $loss_{width}$ wave and in (b) for the $loss_{height}$ wave.

3.3.3 BVP Features

In the Table 3.4 are presented the features computed from the BVP signal. This signal is mostly used as a way to extract HRV [63, 78], however, since HRV features were already computed from the ECG signal, the only HRV features extracted from this signal were statistical ones (Interbeat Interval (IBI) feature).

The BVP statistical features are measures of vasodilation or vasoconstriction. Vasoconstriction is induced by increased sympathetic activity and vasodilation by decreased sympathetic reaction and increased parasympathetic reaction [42]. The mean value of BAV is also an index of vasoconstriction [78]. The BAV and pulse width are correlated with the systemic vascular resistance [67]. Features from the first and second derivatives of the signal are being studied to find its physiological interpretations [67, 78].

Table 3.4: Features extracted from BVP signal. From the features marked with *, statistical parameters are computed.

Feature	**Meaning**
BVP*	Filtered BVP signal
BAV*	BVP peak-to-peak amplitude variation
BVP range	Difference between the maximum and the minimum of the BVP signal
Pulse width*	Time to reach half the maximum value of the BVP peak
Maximum peak time	Time instant where the maximum value of the BVP signal is registed
IBI*	Interval between heartbeats
First derivative	Mean value of the first derivative of the BVP signal
Second derivative	Mean value of the second derivative of the BVP signal
First normalized derivative	Mean value of the first normalized derivative of the BVP signal
Second normalized derivative	Mean value of the second normalized derivative of the BVP signal

3.3.4 Pupillometry Features

Pupil diameter data has been used in several psychophysiological studies [46, 52, 55] since it is a marker of SNS activity. The features extracted from the pupillometry data are presented in the Table 3.5. The 'number of peaks' feature is computed from the pupil diameter data if a peak is registed with a absolute value superior to 0.5 mm. The feature that is introduced in this study, and that is also used to discard uninteresting subjects, is the blinking percentage.

Table 3.5: Features extracted from pupillometry signal. From the features marked with *, mean and standard deviation parameters are computed. Each of these features are computed for the selection, choice and feedback phases of the IGT.

Feature	**Meaning**
Pupil diameter*	Pupil diameter in mm
Pupil diameter variation*	Variation of pupil diameter in mm
Number of peaks	Number of detected peaks superior the the applied threshold
Blink %*	Percentage of time that the subject is blinking or looking away from the screen
AUC*	Area under the pupil diameter curve

3.4 Features Selection and Classification

In this section, the methods used to find the best combination of features that provide the best predictive model of personality and decision making behavior are described. The same methology was applied to the feature selection and classification of all signals for the all scales in study: Agreeableness, Extraversion, Neuroticism, Openness to Experience, Conscientiousness, Maximization and Regret scales. This methodology was chosen because it is the methodology used in the doctoral thesis in which this master's thesis is inserted.

First, the Pearson correlation method was used to eliminate the correlated features. The Pearson correlation coefficient is always a value between -1 and +1, with 0 meaning no correlation and -1 and +1 implying a linear relationship (negative or positive, respectively). Highly correlated features have an absolute coefficient higher than 0.9 [69], so all the extracted features which scored a Pearson correlation absolute coefficient superior to 0.9 were left out.

The applied classification method to compute the best combination of features for each scale was the Ordinary Least Squares (OLS) linear regression, applied with the k-fold cross-validation method. The OLS has as its target to minimize the sum of the squares of the differences between the observed and the predicted values for estimating the unknown intercept and slope parameters of a linear regression model. So a model that fits better the given data is a model with smaller differences between observed and predicted values.

To evaluate the precision of the prediction model to a data set previously unknown to the model, the k-fold cross-validation method was used. This method randomly divides the data in exclusive k sets, usually of the same size, and, iteratively, uses each one as test and the remaining population are utilized to train the model. With this method, every observation will be used for training and validating the model and each observation will be only tested once.

In Figure 3.9 are presented the steps to obtain the model with the best features combination. The different populations groups, which are split in train and test subsets, are general assigned from pA to pZ.

Each population will advance, individually, to a feature selection block, where each feature will be used to classify the scale to predict and the error of this prediction will be calculated. The first iteration will return a feature for each population (from fA to fZ), which corresponds to the feature with the lowest error. Therefore, the frequency of each feature is calculated to attribute the best feature for the entire population and the best feature will be the one that repeats itself more than the others. This result (frs) will then again enter the feature selection block and will be validated in combination with all the remaining features to find the best combination of two features. This process will continue until all features are analysed. Taking into account that the population is randomly distributed, the results will also differ when the random state is changed.

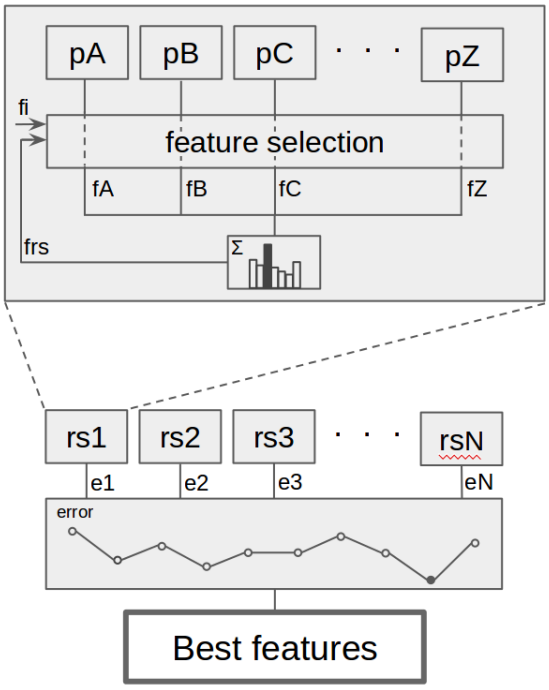

Figure 3.9: Steps involved in feature selection and classification to define the predictive model of personality and decision making behavior.

To solve this problem, the last procedure is repeated (rs1 to rsN) attributing a different seed each time. Twenty random seeds were used and the chosen model of prediction corresponded to the one with the lowest error.

The error above mentioned to perform the evaluation of the classifier is made using three parameters that together are used to calculate the model error. Thus, the Root Mean Squared Deviation (RMSD), the bias and the slope deviance extracted from the obtained linear regression are used to evaluate the accuracy of the classification of the testing set. The *RMSD* is calculated using equation 3.8, where N is the number of people of the testing set, p is the value predicted by the classifier and the o is the real classification of the person. The *bias* calculation is presented in equation 3.9, where $\overline{p}$ is the mean of the predicted values. The *slope* error is based on the angle difference between the desired linear regression and the obtained one. Piñeiro and colleagues proved that, in order to correctly estimate the regression parameters, the observed values should be in the y-axis and the predicted values in the x-axis [49]. The desired linear regression has a slope equal to 1 and intercepts the y-axis in 0.

$$RMSD = \sqrt{\frac{1}{N-1}\sum_{i=1}^{N}(p_i - o_i)^2} \tag{3.8}$$

$$bias = \sqrt{\frac{1}{N-1}\sum_{i=1}^{N}(o_i - \overline{p})^2} \tag{3.9}$$

Thus the error of each model is represented by the formula $model\ error = RMSD + slope + bias$.

3.5 Personality Questionnaires

Both personality and decision making behaviour scales were measured through the online survey and each item of the questionnaires presents as an answer a standard five-point Likert-like scale, where 1 corresponds to 'completely disagree' and 5 to 'completely agree'. Therefore, a high score for example in the Regret scale corresponds to a person that experiences more regret when presented with the consequences of poor decision-making. Some items scores, for instance from the Regret scale the 'Once I make a decision, I don't look back.' item, have to be inverted prior to the calculation of the result of the each questionnaire. The result is given by the average of the answers to each scale items.

The Maximization and Regret scales have 13 and 5 items each, respectively. The NEO-FFI has 60 items, 12 for each personality dimension.

Chapter 4

Experiment

This chapter describes the performed experiment: its phases, the IGT description and specific alterations made for this study, the process of participants recruitment, the population characterization and lastly the data acquisition conditions.

4.1 Experiment Description

As the main objective of this thesis is to verify the impact of personality in the decision making behavior through the measurement of PS, it was necessary the realization of a task that simulates real life decision making. The IGT is one of the most widely explored psychological tasks that simulates an environment of everyday decision making where the decisions are made under uncertainty or ambiguity [9]. This means that when a person has to make a decision, the possible outcomes of that decision or the probability of getting a reward or punishment are unknown. It is a card game where we have four decks that are randomly placed on the screen and all of them differ in the quantities of money that we can receive or lose. The decks differ in terms of the amount of money that could be lost or won. The frequency of reward and punishment is also different and unknown to the player. The game begins by giving us a fictitious amount of money that the player should increase as much as possible. It has 100 trials and in each one of them the player has to choose a card and after that is provided with the feedback of its choice. With the feedback of the money lost or won given after each trial, the player should conclude that the decks associated with a high gain are associated with a high loss and the decks with low gain are associated with a low loss, so the latter are more advantageous in the long run [9, 75].

For the participants begin to understand the mechanics of the task, they will perform two test trials that work as an experimental phase and do not count towards the 100 trials

of the task. In the beginning of each trial, the participant is instructed to focus on the fixation cross that appears on the screen. After this, the four decks of cards are shown and the participant is told to choose a card by clicking with the mouse on the corresponding deck. In the last phase of the trial, the reward and punishment is shown as feedback to the user. Participants start with 2000 Swiss Francs and are informed that they should maximize their winnings and that they can switch between decks anytime they desire. They are unaware of how many trials the task has, as well as the money that they can earn or lose by choosing each deck.

For this study, some alterations were introduced to the structure of the task. To acquire eye-tracking data, the IGT decks were distributed differently on the screen: two at the top and two at the bottom. Figure 4.1 has a screenshot of the decks disposition. To synchronize the physiological data with the events occurring in the task, the beginning time of each trial was recorded (fixation time), as well as the instant the person chooses the deck (choice time) and the instant where the feedback is given (feedback time). The selection time (time interval between the fixation time and the choice time) corresponds to the time the person spends to select which deck to choose. If the person takes more than 7 s to choose, the trial is restarted. The choice interval and the feedback interval have a fixed time interval of 1.5 s so that changes in the physiological data can be detected.

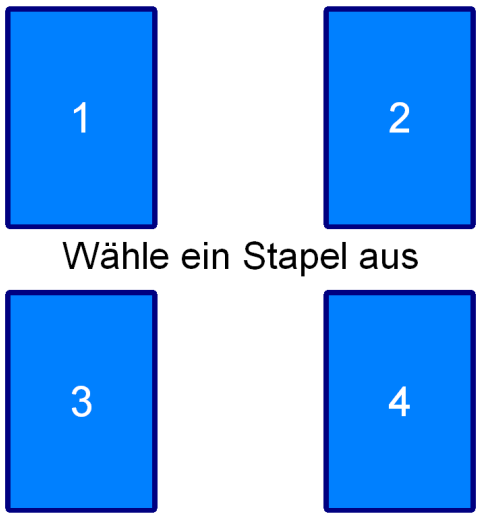

Figure 4.1: Screenshot of the IGT on the deck selection phase.

The experiment has three phases: initially the demographic data and the written consent of every subject was collected, secondly the subjects biosignals are recorded during the realization of the IGT and the last phase corresponds to the personality assessment that is made recurring to an online survey tool.

Each participant gave written permission for their data to be used in this study according to the guidelines of the Declaration of Helsinki for research involving human subjects.

The data acquisition was made in a quiet, sound-attenuated and dimly lit room without vigilance and started being record before the beginning of the experiment so that the subject could adapt to the room environment and the biosignal monitoring.

The German-language version of the NEO-FFI, developed by Borkenau and Ostendorf [8], was utilized to assess the FFM personality dimensions. The Maximization and Regret Scales questionaires, translated and validated by Greifeneder and Betsch for the German language [32], were used to assess maximizing and regret behavior.

After this, the acquired data was offline processed with the aim of extracting features from each signal that could predict personality and decision making behavior.

4.2 Participants

The necessary requirements to participate in this study were:

- Being healthy
- Have normal, or corrected-to-normal, vision
- Not having a medical history of neurological or psychiatric illnesses
- Not being currently being medicated
- Being fluent or native speakers of Standard German

All volunteers were consistently right-handed [2].

The participants are psychologists, that were recruited using a mailing list, or university students from areas such as technology, engineering and economics. These students are from the Swiss Federal Institute of Technology and the University of Zurich. They were paid with 20 Swiss Francs, or the equivalent in Euros, or in the case of psychologists, with hours.

4.3 Data Acquisition

The data acquisition was done through in-house done software, coded in Python language, that connects the Biosignalsplux device, the eyetracker device and the IGT program. This software returns a file with all the acquired data. The acquisition was made in the Department of Psychology of the University of Zurich. EDA, ECG and BVP were acquired with the Biosignalsplux with a fs = 1000 Hz and the eyetracking data with a fs = 60 Hz. The number of bits used in this thesis was 12 bits for each channel of the Biosignalsplux ADC.

The EDA electrodes were placed over the left hand palm since the palms are one of the places with the highest percentage of sweats glands of the human body [10] and the participants are consistently right-handed. The BVP sensor was placed on the index finger of the left hand and the ECG electrodes on the chest of the participant. Ag/AgCl electrodes with surface diameter of 7 mm were used in EDA and ECG acquisitions.

Chapter 5

Results and Discussion

In this chapter, the results of this thesis are presented and discussed. Initially, the population is described and the results of the personality questionnaires are presented. Then, the results of the biosignals processing and feature extraction are displayed. To conclude, the predictive models of personality for each biosignal and for the combination of them are presented and discussed.

5.1 Description of the Population

For this study, a total of 71 volunteers (18 male and 53 female) were used. The youngest person to complete the gambling task was 16 and the oldest 34 years old (Mean (M) = 23.9; Standard Deviation (SD) = 4.2 years).

Some subjects only have one, two or three of the four recorded signals due to presence of artifacts in the signals. This is probably due to the fact that, during the task, people sweat and the electrodes are displaced. Table 5.1 presents the physiological data available from each subject. Twenty-four out of seventy-one subjects had available data from all four biosignals. The average duration of the collected data during the realization of the task was M = 548.5 (SD = 46.2) s, the longest being 699.0 s and the shortest 490.0 s.

Figure 5.1 presents a violin plot with the results of the questionnaires for all the studied personality scales. Looking at the population distribution, it is possible to conclude that most scales results present a a shape similar to a gaussian curve. This means that there are few people classified as high and low scorers on these scales. Most people scored a value from 1 to 4 in the Neuroticism, Maximization and Regret scales. In the Openness to Experience and Conscientiousness scales, the majority of the population scores values are above 3, which means that there are few low scorers. The majority of the population was classified with values between 3 and 4 in the Extraversion and Agreeableness scales.

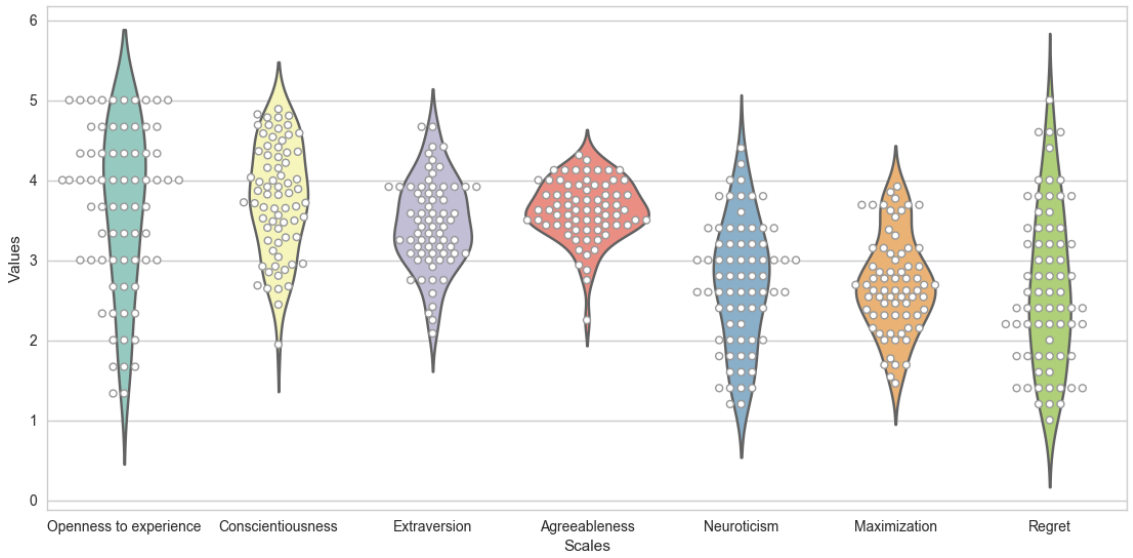

Figure 5.1: Violin plot with the results of the personality questionnaires. The white dots represent the precise result of each person.

The mean average values were M = 3.65 (SD = 1.03) for Openness to experience, M = 3.77 (SD = 0.69) for Conscientiousness, M = 3.45 (SD = 0.55) for Extraversion, M = 3.63 (SD = 0.37) for Agreeableness and M = 2.72 (SD = 0.77) for Neuroticism. For the Maximization and Regret scales the mean average values were M = 2.70 (SD = 0.60) and M = 2.66 (SD = 0.97), respectively.

Table 5.1: Physiological data used in the study. Subjects whom no physiological signals were used were omitted. The data marked with a X is available.

Subject	EDA	ECG	BVP	Pupil	Subject	EDA	ECG	BVP	Pupil
2	X	X	X	X	42	X	X	X	X
3	X	X		X	43		X	X	X
4	X	X	X	X	44	X	X		X
5	X	X	X	X	46	X	X	X	
6	X	X	X	X	47		X	X	X
7	X	X	X	X	48	X	X		X
8	X	X		X	50	X	X	X	X
9				X	52	X			X
10				X	53	X			X
11				X	54	X			X
12				X	55	X			
13				X	57	X			X
16	X				59	X	X	X	X
17	X			X	60	X	X	X	X
18	X	X	X	X	61	X	X	X	X
19	X	X	X	X	62	X	X		X
20	X	X	X	X	63	X	X		X
21	X			X	64	X	X	X	X
22	X			X	65	X	X	X	X
23				X	66	X	X		X
24	X			X	67	X	X		X
25	X			X	68	X	X	X	X
26	X			X	69	X	X		X
27	X			X	70		X	X	X
28	X			X	71	X	X	X	X
29	X			X	72	X	X	X	X
30	X			X	73	X	X	X	X
31	X	X	X	X	74	X	X	X	X
33		X		X	75		X		X
34	X	X	X	X	76		X	X	X
35	X	X	X	X	78		X	X	X
36	X	X		X	79		X		X
37	X	X		X	80		X	X	X
38	X	X		X	81		X	X	X
39	X	X	X	X	82		X		
40	X	X		X	Total	54	49	32	67

5.2 Biosignals Processing and Feature Extraction

The first steps to predict personality through biosignals, presented in the sections 3.2 and 3.3, involved processing tools to extract features from ECG, EDA, BVP and pupillometry. The results obtained are presented in this section.

5.2.1 ECG

In Figure 5.2, the first plot represents the filtered ECG signal of a subject from our study with the QRS complexes detected through the Pan-Tompkins algorithm, marked with black dots. This algorithm proved to be assertive in the detection of QRS complexes. In the second plot, the HRV signal for the same time interval of the ECG represented on the first plot, is also exhibited. As can be seen in Table 5.1, from the 71 study participants, only 49 overcame the outlier detection criteria of the RR intervals.

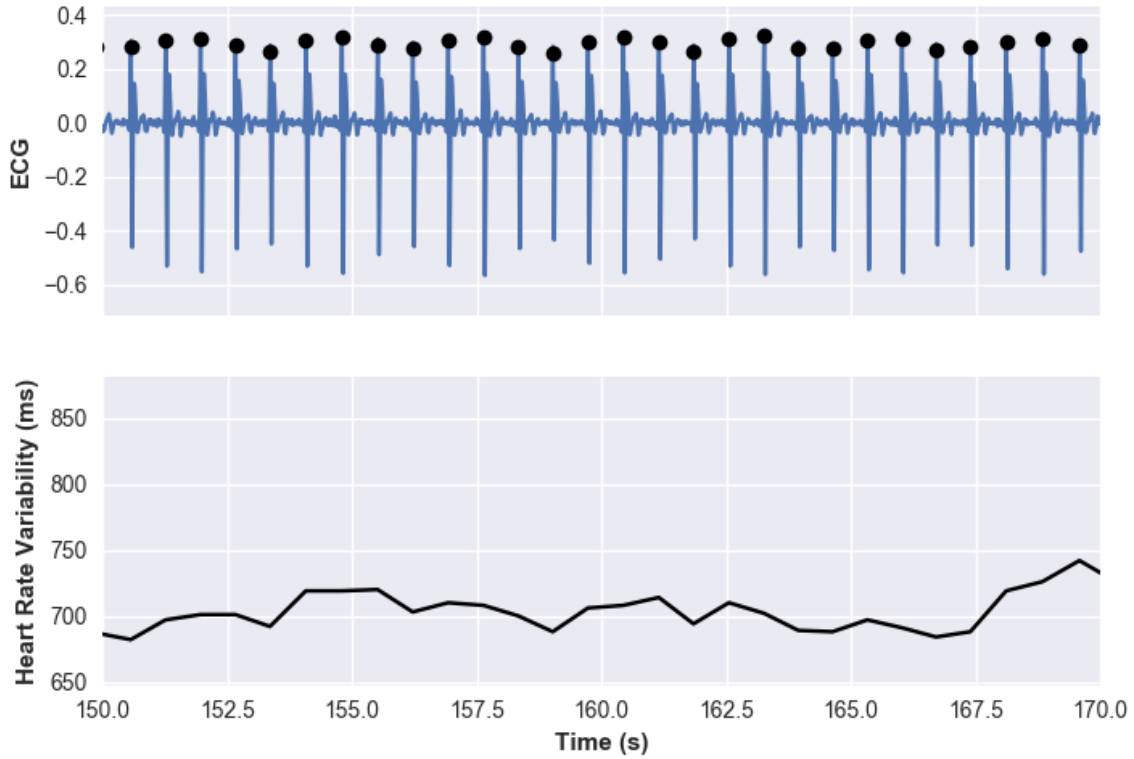

Figure 5.2: In the first plot is presented the ECG signal from a subject of the study. The detected QRS complexes are marked with a black dot in the ECG plot. The HRV, for the same time interval, is presented in the second plot.

In the plot 5.3a, it is represented the histogram from the HRV. In orange are marked the computed linear regressions that approximate the triangular shape of the histogram. The regression with positive slope was calculated taking into account the values on the left of the mode value of the histogram while the one with negative slope took into account the values on the right. The interception of these regressions with the x-axis is used to calculate the TINN. In the plot 5.3b, it is presented the histogram of the absolute

successive differences between RR intervals and in orange the negative exponential curve that best fits this histogram. The number of bins used was chosen empirically, since no specific value was found in literature, and the same value, 25, was applied to the histogram of all subjects. The approximation to the histogram through the exponential curve, $ke^{-\phi x}$, was done so that its coefficient of decay, ϕ, could be used as a feature. The k parameter is related to the scaling of the curve. The Poincaré plot in Figure 5.3c has marked with a black line and a black dashed line the major and minor semi-axes of the ellipse that best fits the data. These correspond to the SD1 and SD2 features that are correlated with short-term and long term variability. In the plot 5.3d, it is represented the PSD estimation in function of the frequencies present in the HRV signal. All features related to the frequency domain are extracted from this plot.

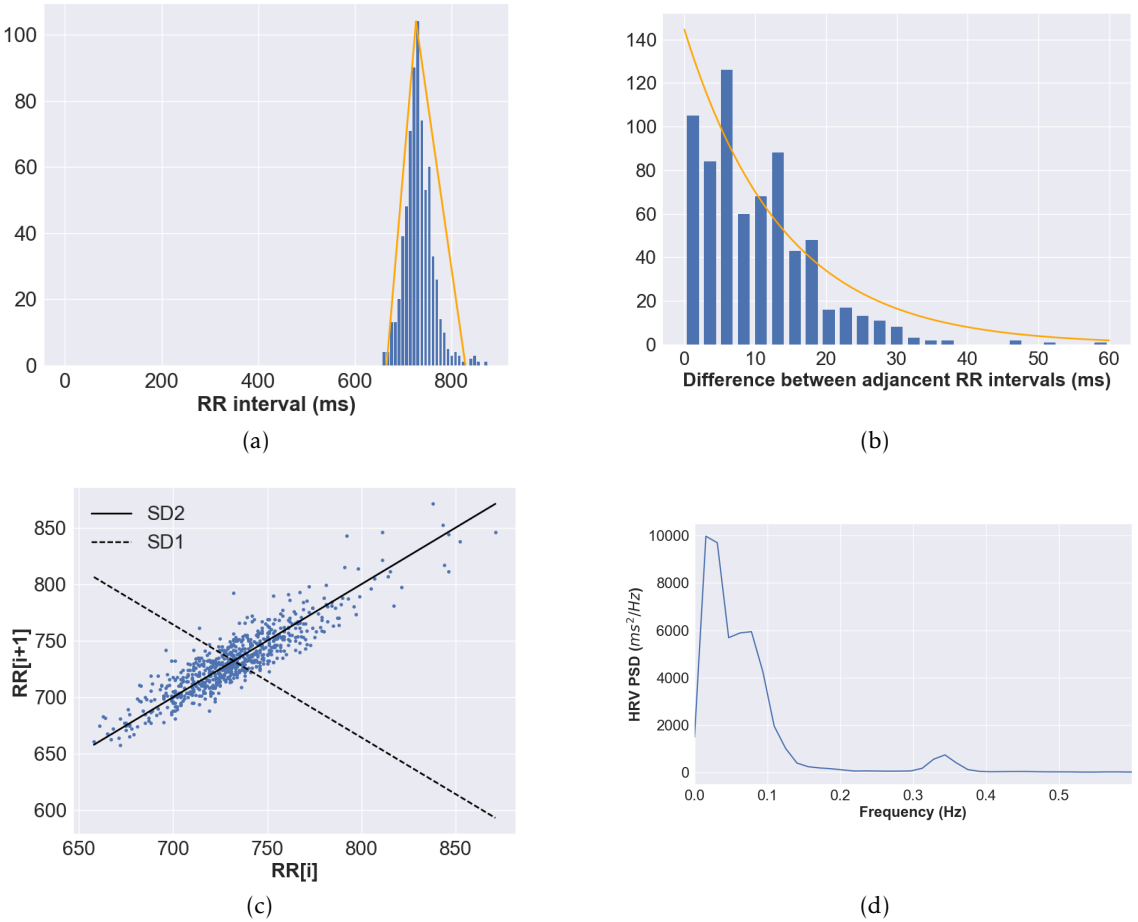

Figure 5.3: All data presented in this plots belongs to a subject of this study. (a) HRV histogram with its triangular interpolation marked with the orange lines; (b) Histogram of the sucessive differences of HRV with the exponential curve marked with a orange line; (c) Poincaré plot with SD1 marked with a black dashed line and SD2 marked with a black line; (d) PSD estimation plotted in function of the frequencies.

The total number of extracted ECG features is 258.

5.2.2 EDA

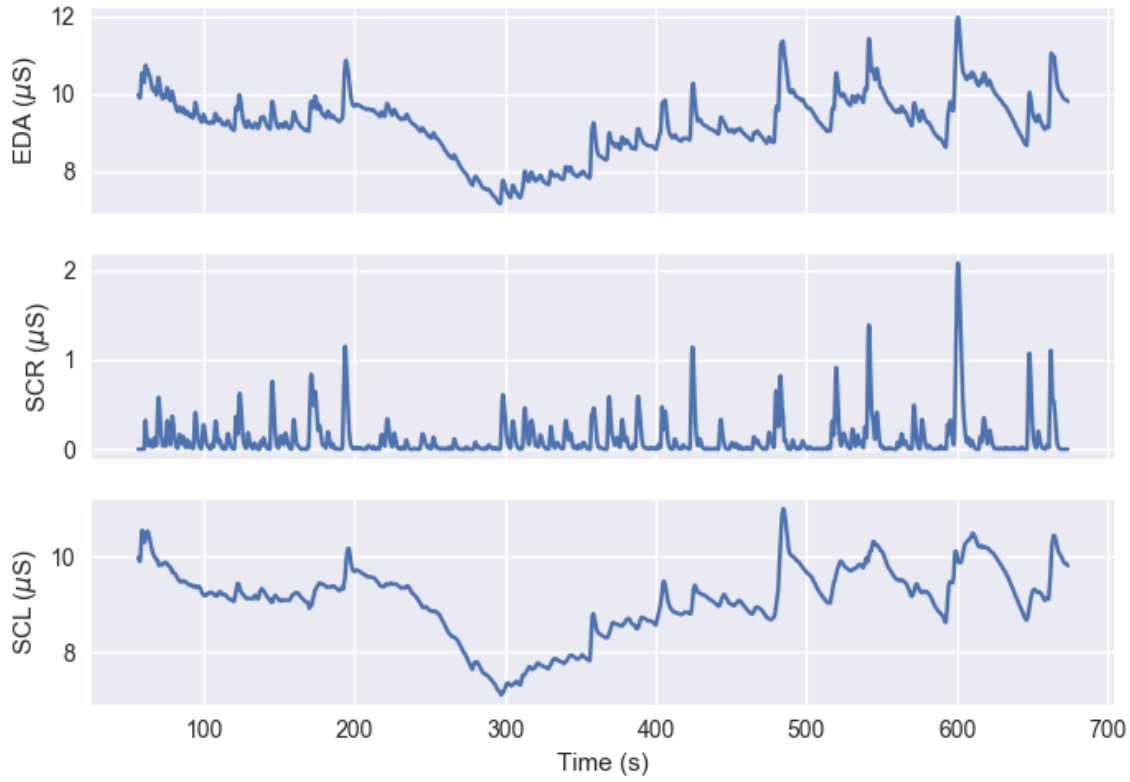

Figure 5.4: EDA signal and respetive components: the SCR are presented in the second plot and the SCL in the third plot.

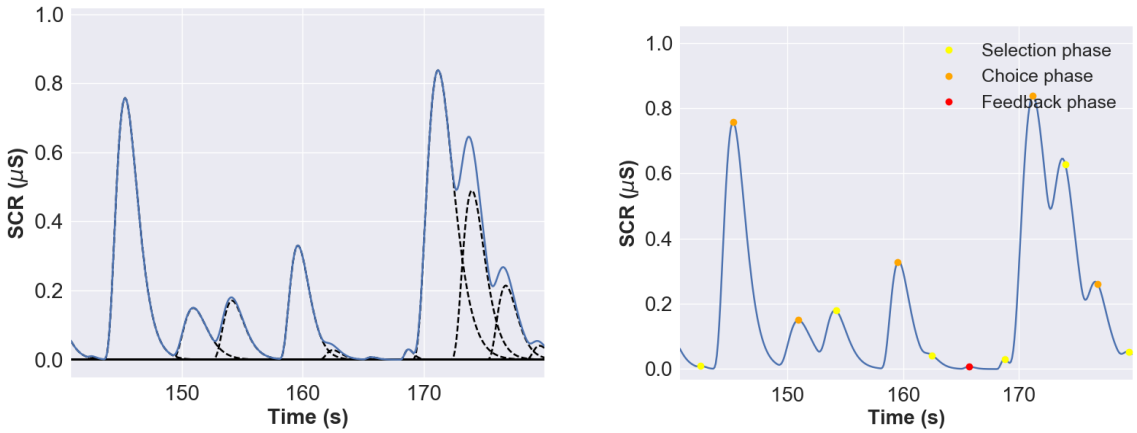

(a) (b)

Figure 5.5: Segment of the SCR component of the EDA signal of a subject from the study: (a) in blue is the sum of the detected SCR and in black dashed lines are marked each individual event detected by the model; (b) through SCR component and the synchronization with the IGT, it is possible to identify in which phase each peak occured.

In the Figure 5.4, the first plot presents an example of a filtered EDA signal from a subject of the study. In the second and third plots are represented the SCR and SCL

components of the signal, extracted from the EDA signal according to the model described in section 3.2.2. Statistical features of SCL were extracted from the signal presented in the third plot and the features related to the SCR, such as the its amplitude and rise time, were extracted from each individual SCR.

In Figure 5.5a, it is possible to verify the efficiency of the implemented model - overlapping SCR in increasing and decreasing zones are detected as well as small amplitude events. Its utility to extract features, such as the number of peaks that occur in specific times of the IGT, concretely the selection, choice and feedback pases, is shown in the Figure 5.5b.

The total number of features extracted from the EDA signal are 189.

5.2.3 BVP

In Figure 5.6, in the first plot, it is represented the SSF signal computed from the BVP signal from subject 2. The SSF peaks onset, marked with green dots, and the peaks maximum, with orange dots, were extracted according to the methodology presented in section 3.2.3 with the objective of identifying the onset and maximum of the BVP peaks. In the second plot, it is represented the filtered BVP signal with its peaks onset and maximum identified with green and red dots, respectively.

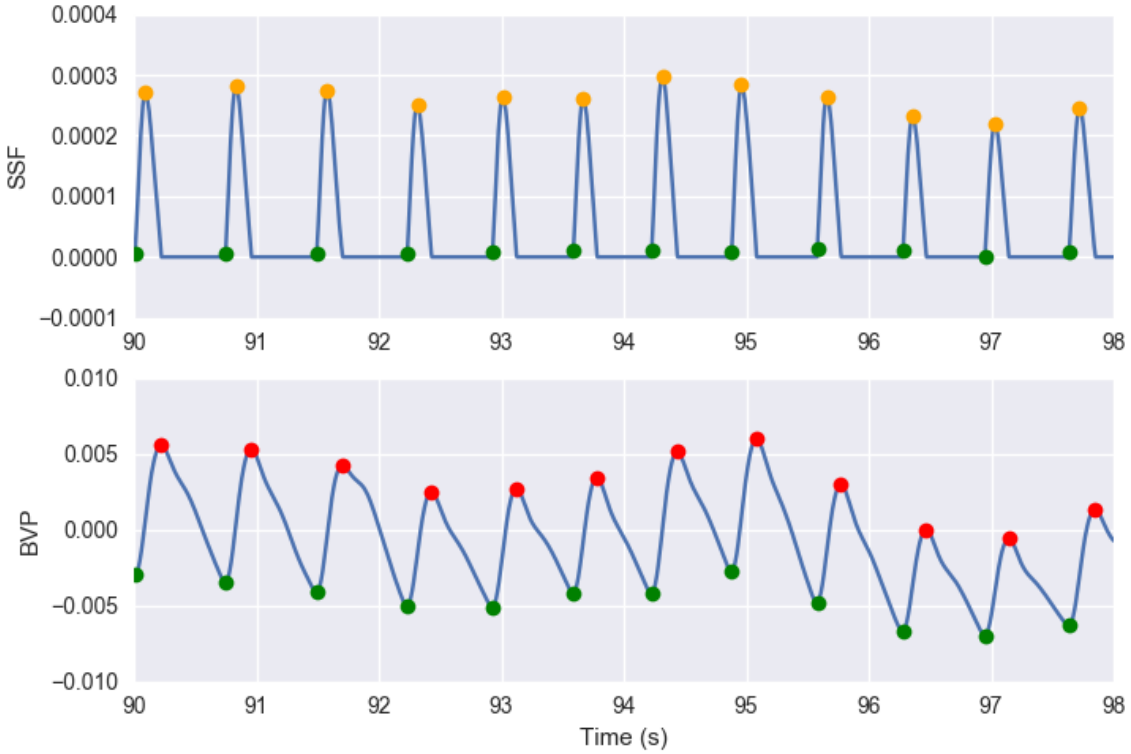

Figure 5.6: BVP signal from a subject of the study: the SSF signal with the peaks onset and maximum marked with green and orange dots is in the top plot. In the bottom plot, the filtered BVP signal is shown with its peaks onset and maximum, computed through the SSF signal, marked with green and red dots.

This methodology of processing the BVP signal revealed itself useful for the extraction of features since it could easily detect the peaks maximum and onset.

The total number of features extracted from BVP is 127.

5.2.4 Pupillometry

In Figure 5.7, it is presented the pupil diameter during the performance of the first trial of the IGT. Each plot corresponds to the selection, choice and feedback phases of the IGT, respectively. The number of detected peaks in each plot is zero since in this trial no peak exceeded the peaks detection criterion. The times where the signal is equal to zero correspond to the times when the subject is blinking or looking away from the screen. All features, except the blink percentage, are calculated after these zeros are excluded from the signal.

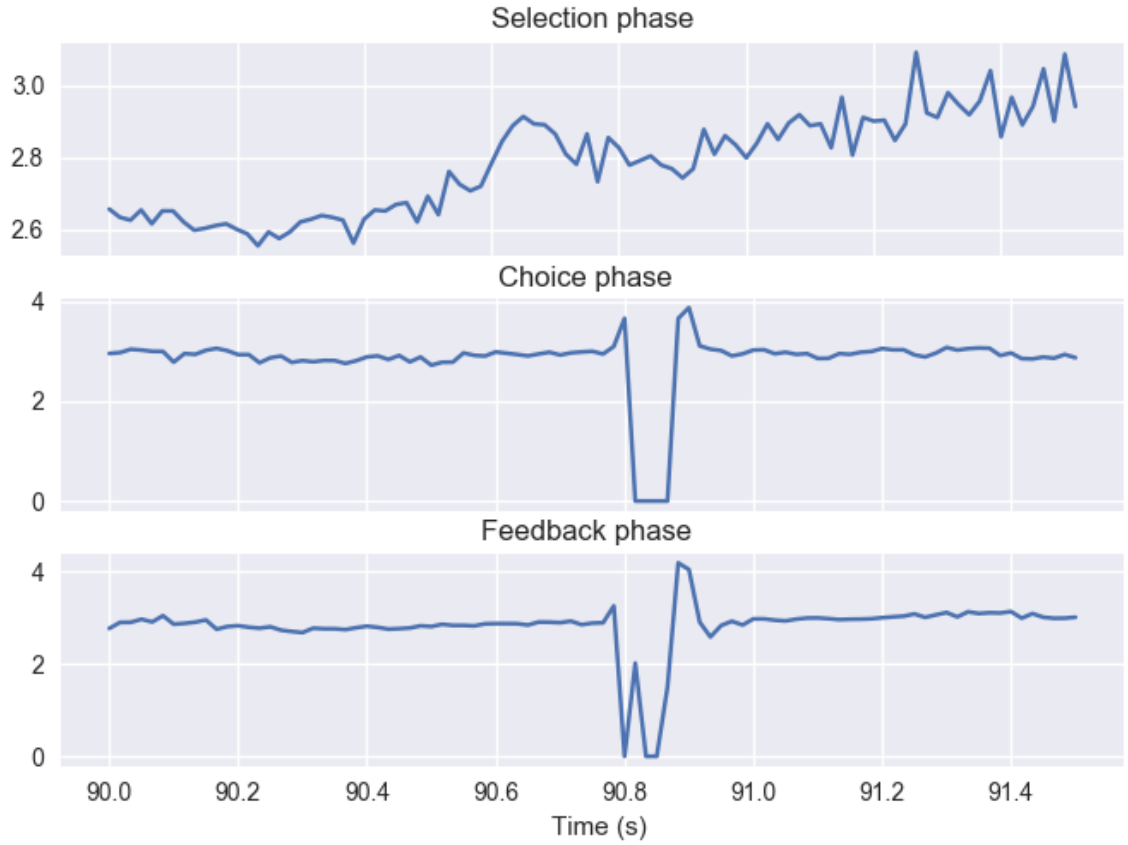

Figure 5.7: Pupil diameter during the first trial of IGT, measured in mm, of a subject of the study: in the first plot, the pupil diameter during the selection phase is presented, in the second is the diameter during the choice phase and the last plot has the pupil diameter during feedback.

The total number of features extracted from the pupillometry data is 162.

5.3 Analysis of Predictive Models

The first step of feature selection, used to eliminate highly correlated features, consisted in computing the Pearson correlation coefficient between all features and exclude the ones which scored an absolute coefficient greater than 0.9. In Figure 5.8, it is represented a barplot in blue with the number of features from each signal and one with the features from all signals, prior to the feature selection, and the orange bars represent the number of features after the application of the Pearson correlation coefficient. Only the number of features from ECG did not decrease to less than half the initial number of features. With the exclusion of these highly correlated features, the computational time of the predictive models has greatly decreased since, as explained in section 3.4, the model used in this thesis analyzes all features to find the best combination.

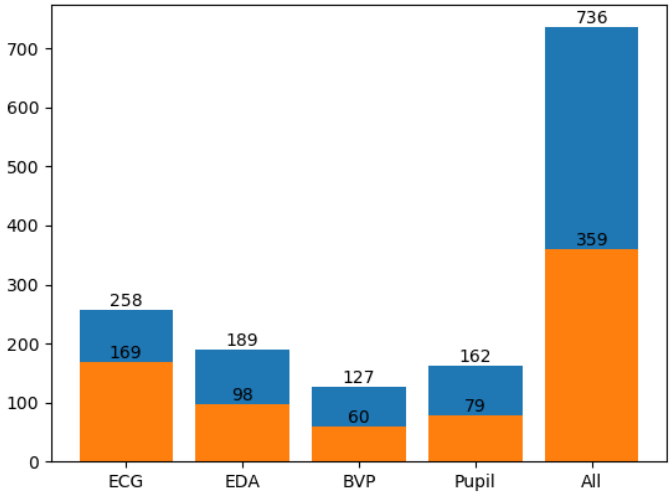

Figure 5.8: Barplot with the number of features extracted from each signal and the total of features from the four used biosignals, in blue bars, and the number of features after the feature selection with the Pearson correlation, in orange bars.

To find the optimal personality predictive models the best combination of features was selected through the model shown in Figure 3.9 and explained in section 3.4. In this thesis a k-fold method with a k = 10 was chosen So, the population was divided in 10 exclusive sets and each one was used once as testing set, with the remaining population being used to train the model. Since the population was divided in 10 sets, 10% of the number of participants with available data for each signal are chosen to be part of the testing set. The testing sets for the ECG were composed by 4 or 5 people since there was data from 49 subjects. For the EDA were composed by 5 or 6 people since the data of 54 participants was available. The testing sets for the BVP had 3 or 4 people since there was only data from 32 subjects and for the pupillometry data the testing sets were composed by 6 or 7 people. For the models constructed with the features from all signals, 2 or 3

people were used as testing set since there was only 24 participants with data available from all biosignals.

5.3.1 ECG Model

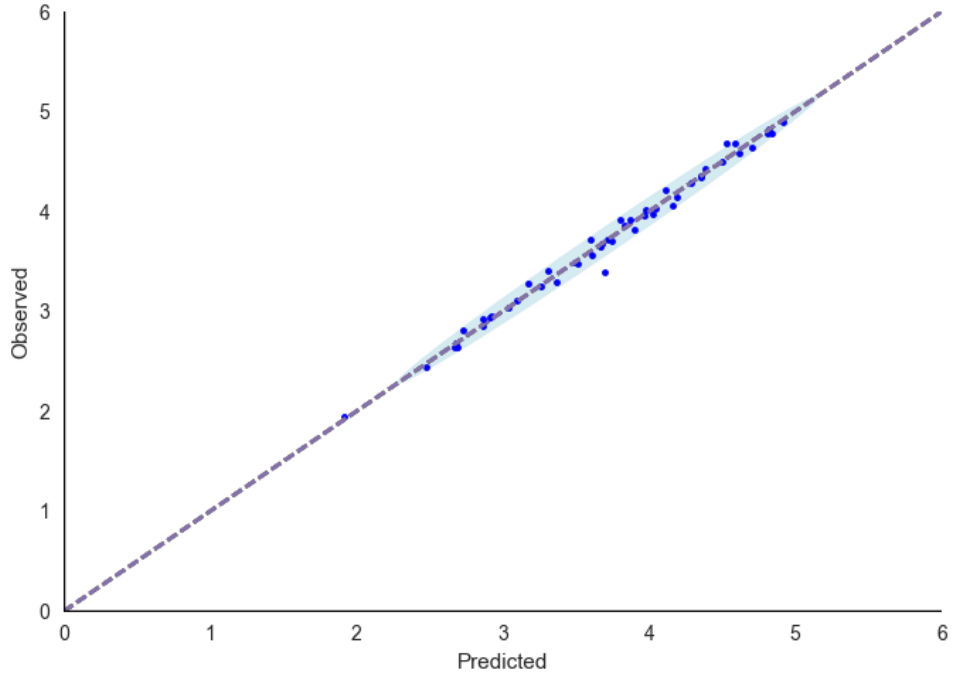

Figure 5.9: Predictive model result for the Conscientiousness scale, obtained with features from ECG.

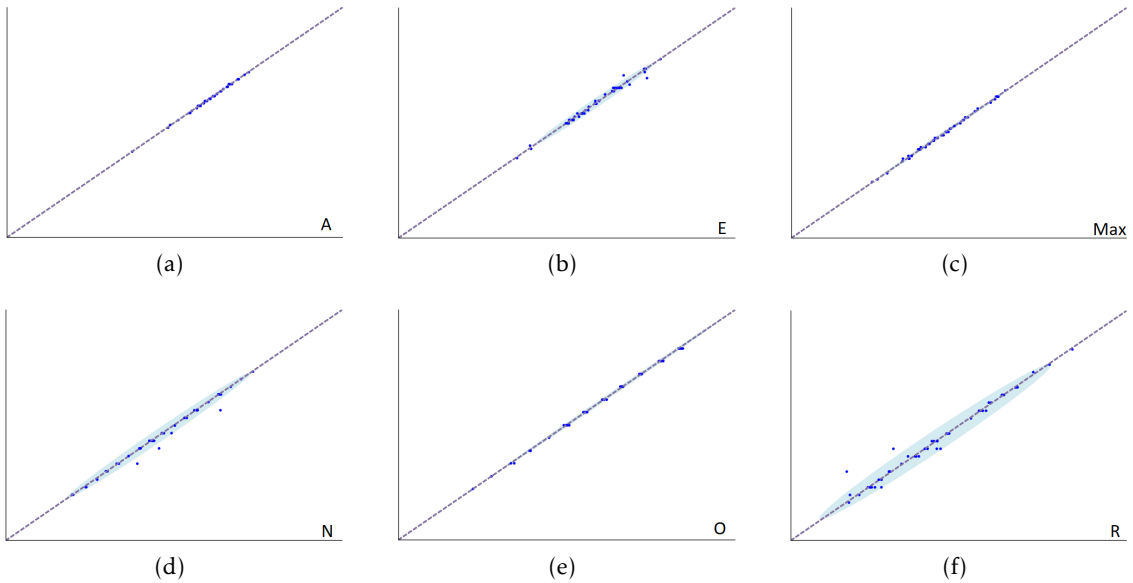

(a) (b) (c)

(d) (e) (f)

Figure 5.10: Predictive model results for Agreeableness (A), Extraversion (E), Maximization (Max), Neuroticism (N), Openness to Experience (O) and Regret (R), obtained with features from ECG.

The results obtained for the best combination of features from the ECG signal for each personality scale are represented in the Figures 5.9 and 5.10. The value given by the personality questionnaires corresponds to the vertical axis of each plot and the prediction given by the classifier to the horizontal axis. Each blue dot represents one subject from the testing set and the blue dashed line represents the perfect predictive model, in which the linear regression has a slope of 1 and intercepts the vertical axis on 0. The light blue ellipse shows the 95% confidence region of the data. This ellipse is calculated through the covariance of the data and shows the region where 95% of the data samples are located according to their Gaussian distribution.

Resorting only to a visual inspection of the results, it is possible to conclude that most predicted values are very close to what was expected from the questionnaires. This means that the predictive model is classifying this study population in the correct way. Using only ECG features, Agreeableness, Maximization and Openness to Experience are the models which perform best compared with the other results and the worst performance belongs to the Regret scale.

Table 5.2: Results of the performance of the predictive model with ECG features: for each scale is presented the number of features used by the classifier, the best five features of each model, the model error and the mean error of the absolute differences between the predicted and the observed values.

Scale	Number of features	Best five features	Model error	Prediction error
O	42	*b2 - % LF, b1 - ApEn, b2 - % VLF, b1 - LF peak, b5 - LF/HF*	1.02	0.010 ± 0.009
C	43	*b3 - maximum HR, b4 - LF peak, b5 - LLE, b5 - % LF, b2 - LF peak*	0.79	0.05 ± 0.05
E	42	*b1 - SampEn, b1 - LF peak, b1 - HF, b4 - HRV triangular index, b3 - LF_{nu}*	0.60	0.04 ± 0.05
A	42	*b5 - HF peak, tt - LF peak, b1 - SD1/SD2, b4 LF peak, b2 - LLE*	0.41	0.02 ± 0.02
N	42	*b1 - HF peak, b2 - % VLF, b5 - % VLF, b1 - LLE, b3 - minimum HR*	0.91	0.04 ± 0.09
Max	42	*b1 - HF peak, b3 - SD1/SD2, tt - LF peak, b4 - LF peak, b3 - Autocorrelation*	0.62	0.02 ± 0.02
R	42	*b5 - SampEn, b5 - HF peak, b4 - ApEn, tt - LLE, b1 - ϕ*	1.17	0.1 ± 0.1

In Table 5.2 are presented the results of the evaluation of the model performance for each scale. Through this table, it is possible to see that all scales need less than 44 features to minimize the model error. In the last column of the table is presented the prediction error, which measures the mean error of the absolute differences between the predicted

and the observed values. Therefore, all models should have a prediction error as close to 0 as possible. With that in mind, the scales which present the best results are the Openness to Experience, Agreeableness and Maximization scales with prediction errors of 0.01, 0.02 and 0.02, respectively. Although the model for the scale of Neuroticism presents a low prediction error, it presents the highest standard deviation value, meaning that the prediction error values are spread out over a wider range of values. The prediction error for all scales is inferior to 0.1, except for the Regret scale. Thus, these results confirmed the initial expectations obtained from the visualization of Figures 5.9 and 5.10. The intrinsic model error should also have a value as close to 0 as possible. As expected, the Agreeableness and Maximization models have the lowest model error and Regret the highest. The Openness to Experience scale despite presenting the lowest prediction error has associated the second highest model error. This high error is explained by the fact that the model error not only takes into account the difference between the predicted and observed values but also the bias of the data and the difference between the slope of the desired linear regression and the one that was obtained.

Also in Table 5.2, the best five features of each model are presented with 28 from 35 of them being different from each other, which leads to the conclusion that each scale is based on specific features. The features that start by the letters *tt* are extracted from the entire task, while the features that start with a *b* are from one of the blocks in which the IGT is divided. The *b4 - LF peak* is the most chosen feature, being present in Conscientiousness (2nd best), Maximization (4th best) and Agreeableness scales (4th best). *b1 - LF peak*, *b2 - % VLF*, *b1 - HF peak*, *tt - LF peak* and *b5 - HF peak* were chosen twice. The *LF peak* and *HF peak* features are the most chosen features across all personality scales, whether being from a specific block or from the entire task. The Conscientiousness model has 3 out of 5 features related to the low frequencies in the HRV. Since the LF component is in an indicator of the balance between sympathetic and parasympathetic activity, the changes in LF during the decision making process can be related to the Conscientiousness dimension. The presence of features related to the low frequencies are also found in the Openness to Experience, Extraversion, Agreeableness and Maximization scales, so the same conclusion can be drawn. Notably, only three features from the entire task were chosen, the *tt - LF peak* in the Agreeableness and Maximization models and the *tt - LLE* in the Regret model. The three best features from the Extraversion scale are from the Block 1. Most of the best five features of all predictive models from the ECG signal belong to Block 1.

In Table 5.3, the number of features from the the ECG signal selected by the classifier, from each block and from the complete task, are represented. For the Openness to Experience, Extraversion, Neuroticism and Maximization scales, most of the features were chosen from Block 1. The Regret scale predictive model has most features selected from Block 3. The Conscientiousness model uses the same number of features from the Block 3 and Block 5 to make the prediction. The Agreeableness model has 10 features selected from Block 2 and 5. Globally, Block 1 had the greatest number of features selected for all

Table 5.3: Number of features per block used by the classifier to predict each scale, with features extracted from ECG.

Scale	Complete	Block 1	Block 2	Block 3	Block 4	Block 5
O	3	12	7	5	7	8
C	3	6	8	9	8	9
E	4	13	4	5	12	4
A	1	9	10	7	5	10
N	5	11	9	5	5	7
Max	3	11	5	5	9	9
R	7	7	7	10	6	5
	26	69	50	46	52	52

models using ECG features.

With this analysis, it is possible to conclude that Block 1 features are the most utilized in the majority of the scales and the features from the complete task are the least used. Therefore, these results are consistent with the hypothesis that personality traits are more expressed in the beginning of the task, when people are just testing the game and don't know yet the better strategy to succeed.

5.3.2 EDA Model

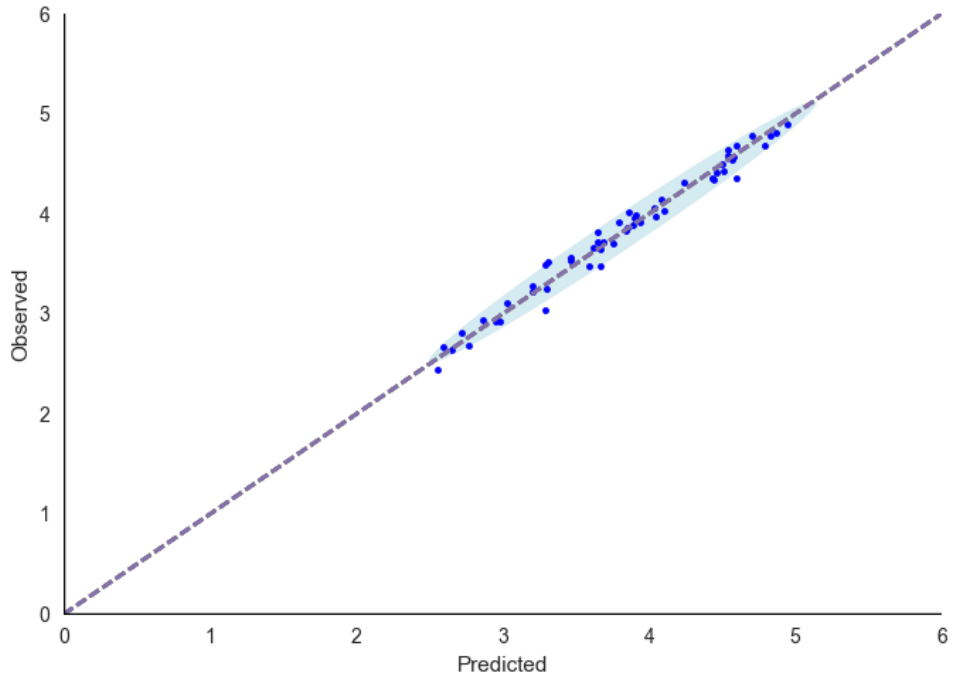

Figure 5.11: Predictive model result for the Conscientiousness scale, obtained with features from EDA.

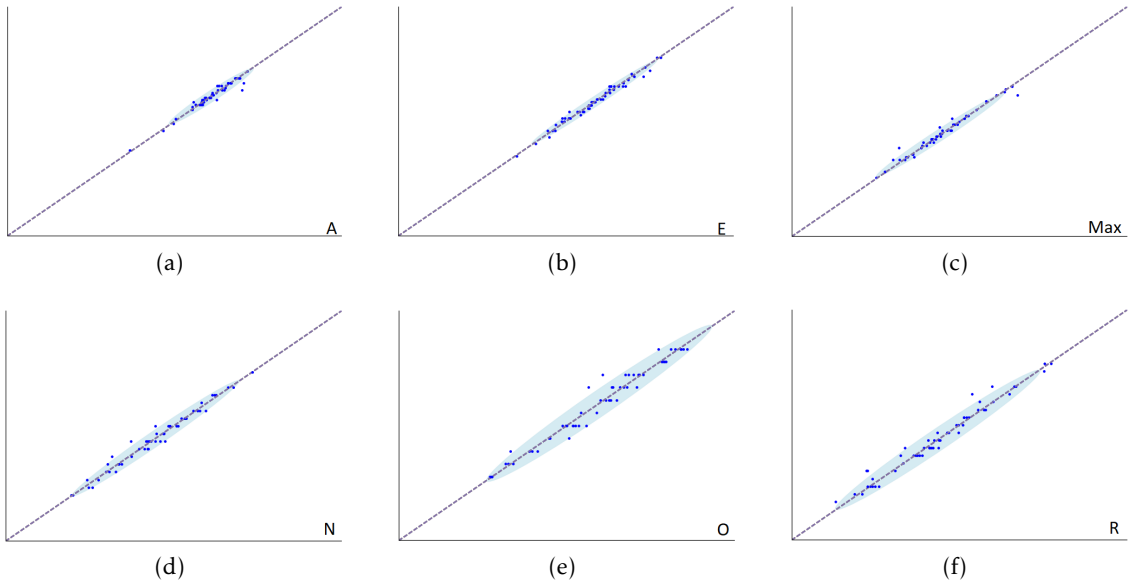

(a) (b) (c) (d) (e) (f)

Figure 5.12: Predictive model results for Agreeableness (A), Extraversion (E), Maximization (Max), Neuroticism (N), Openness to Experience (O) and Regret (R), obtained with features from EDA.

The results obtained for the best combination of features from the EDA signal for each personality scale are represented in the Figures 5.11 and 5.12, with the light blue ellipse presenting the 95% confidence region of the data.

Through visual inspection of the results, it is visible that most predicted values are very close to what was observed. This means that the predictive model is classifying this thesis population in the proper way. Using only EDA features, the models for Agreeableness, Extraversion and Maximization are the ones that perform best and the worst performance belongs to the Openness to Experience scale.

In Table 5.4 are presented the results of the evaluation of the model performance for each scale. Through this table, it is possible to see that all scales need 46 or less features to minimize the model error. The scales which present the best results are the Agreeableness and Maximization scales with a prediction error of 0.05. The prediction error is inferior to 0.1 to all scales except for Openness to Experience and Regret. As expected, the Agreeableness, Extraversion and Maximization models have the lowest model error and Regret the highest. These results verify the initial expectations obtained from the visualization of Figures 5.11 and 5.12.

Also in Table 5.4, the best five features of each model are presented with 29 from 35 of them being different from each other, which makes possible to conclude that each scale is based on specific features. The *b5 - SCR in selection* is the most chosen feature, being present in Neuroticism (1st best), Maximization (2nd best) and Regret scales (1st best). The features *b3 - SCR in selection*, *b1 - SD SCL*, *b5 - maximum SCR peak rate* and *b2 - maximum SCR rise time* were chosen twice. Notably only one feature from the entire task was chosen, the *tt - maximum SCR rise time* in the Neuroticism model. The three best features from the Openness to Experience scale are from the Block 1, while the Conscientiousness model selected three out of the best five features from Block 3 and the Regret model three out of five from the Block 2.

The EDA features that have into account the synchronization with the IGT are chosen sixteen times across all personality scales. These features are the *SCR in selection/-choice/feedback*, that correspond to the ratio between the number of peaks in that phase and the total number of peaks, and also the *sum of peaks height (Correlation with loss)*, *mean of peaks height (Correlation with loss)*, *average of the SCR (Correlation with loss)* and *number of peaks (Correlation with loss)* features. These features correspond to the 'Correlation with loss' features, more specifically the loss wave correlation with the sum of peaks height, mean of peaks height, average of the SCR component and number of peaks functions, respectively. Therefore, the use of more features that take into account not only the changes on the physiological level but also relates these changes with what is happening in the task is encouraged.

The features related to the SCL, SCR amplitude and frequency are present in the Openness to Experience, Extraversion, Neuroticism and Maximization scales. These features are known to be related to sympathetic activity, so it can be concluded that sympathetic activation during IGT performance may be correlated with these personality

Table 5.4: Results of the performance of the predictive model with EDA features: for each scale is presented the number of features used by the classifier, the best five features of each model, the model error and the mean error of the absolute differences between the predicted and the observed values.

Scale	Number of features	Best five features	Model Error	Prediction Error
O	46	*b1 - SCR in choice, b1 - SD SCL, b1 - minimum SCR amplitude, b3 - number of SCR, b2 - number of SCR*	1.22	0.1 ± 0.1
C	46	*b2 - SCR in selection, b3 - SCR in selection, b3 - sum of peaks height (Correlation with loss), b3 - mean of peaks height (Correlation with loss), b4 - number of peaks (Correlation with loss)*	0.75	0.08 ± 0.06
E	46	*b4 - number of SCR, b3 - maximum SCR peak rate, b5 - SD SCL, b2 - SCR in feedback, b5 - maximum SCR peak rate*	0.63	0.06 ± 0.05
A	46	*b2 - maximum SCR rise time, b2 - average of the SCR (Correlation with loss), b3 - SCR in selection, b1 - SD SCR rise time, b1 - maximum SCR rise time*	0.46	0.05 ± 0.07
N	45	*b5 - SCR in selection, b5 - minimum SCR peak rate, b4 - minimum SCR amplitude, tt - maximum SCR rise time, b2 - mean of peaks height (Correlation with loss)*	0.87	0.09 ± 0.08
Max	44	*b1 - SD SCL, b5 - SCR in selection, b5 - maximum SCR peak rate, b2 - minimum SCR peak rate, b1 - SD SCR amplitude*	0.64	0.05 ± 0.08
R	46	*b5 - SCR in selection, b2 - number of peaks (Correlation with loss), b3 - average of the SCR (Correlation with loss), b2 - maximum SCR rise time, b2 - SCR in choice*	1.09	0.1 ± 0.1

scales.

In Table 5.5, the number of features from the EDA signal selected by the classifier, from each block and from the complete task, are represented. For the Openness to Experience, Agreeableness, Neuroticism and Regret scales, most of the features were chosen

from Block 1. The Conscientiousness model uses the same number of features from the complete task and Block 5 to make the prediction. The Extraversion scale has most features selected from Block 3 with the number of features from Block 1 coming in second. The Maximization scale predictive model has most features selected from Block 4. Globally, Block 1 had the greatest number of features selected for all models using EDA features and the features from the entire task were the least used.

From this analysis, Block 1 features are the most utilized features across all of the scales and, thus, the hypothesis that personality traits are more expressed in the beginning of the task is also comproved for the models constructed through EDA features.

Table 5.5: Number of features per block used by the classifier to predict each scale, with features extracted from EDA.

Scale	**Complete**	**Block 1**	**Block 2**	**Block 3**	**Block 4**	**Block 5**
O	5	12	9	7	7	6
C	9	5	8	8	7	9
E	6	9	6	11	6	8
A	7	10	8	8	5	8
N	5	10	7	7	8	8
Max	7	9	5	4	10	9
R	5	10	9	9	6	7
	44	65	52	54	49	55

5.3.3 BVP Model

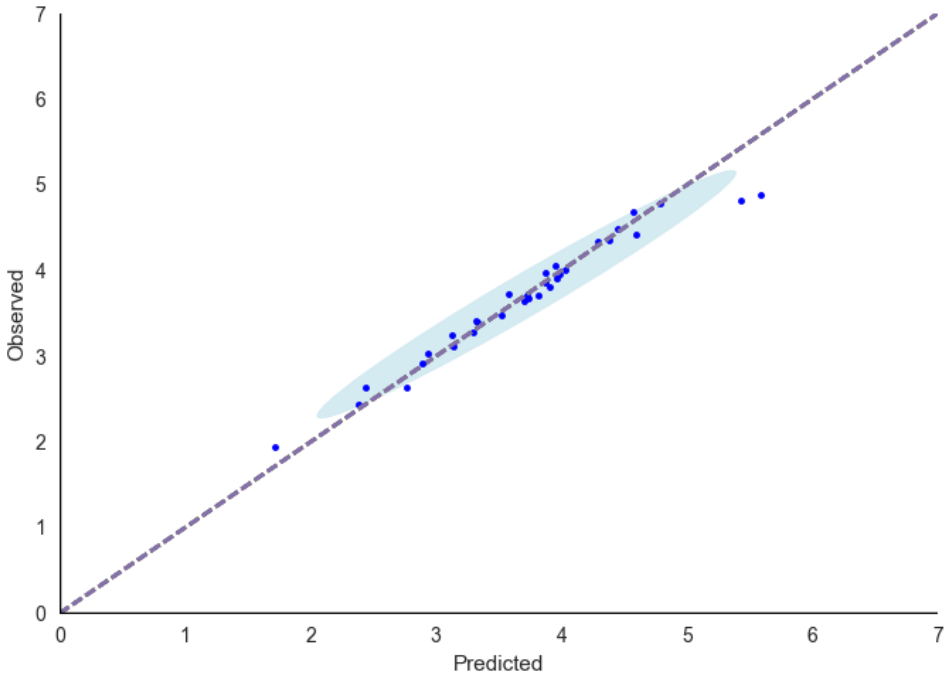

Figure 5.13: Predictive model result for the Conscientiousness scale, obtained with features from BVP.

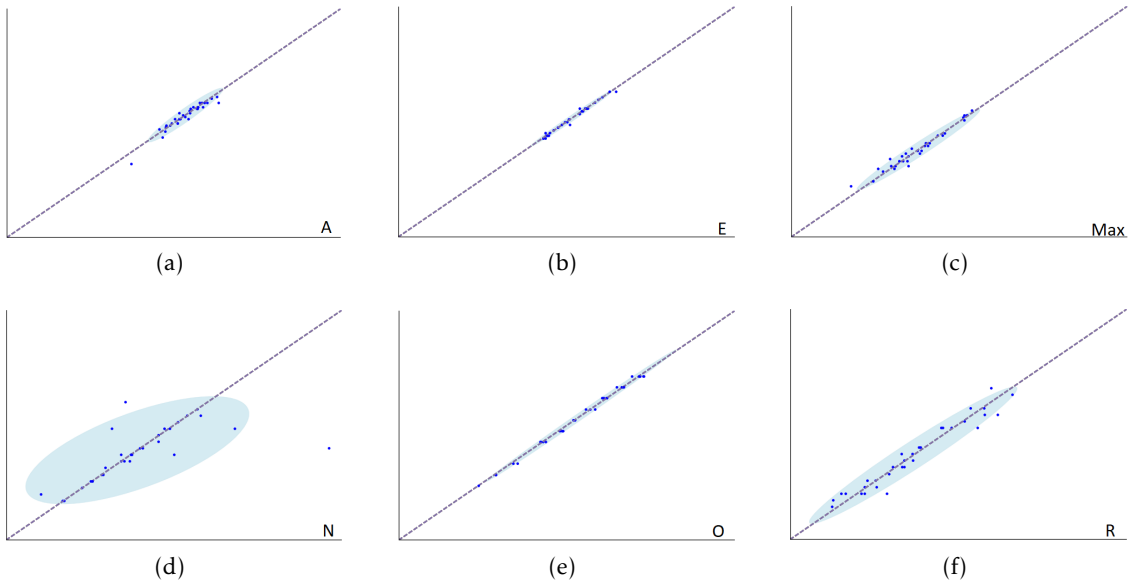

(a) (b) (c)

(d) (e) (f)

Figure 5.14: Predictive model results for Agreeableness (A), Extraversion (E), Maximization (Max), Neuroticism (N), Openness to Experience (O) and Regret (R), obtained with features from BVP.

The results retrieved from the best combination of features of the BVP signal for each personality scale are represented in the Figures 5.13 and 5.14, with the light blue ellipse representing the 95% confidence region of the data.

From an initial visual inspection, it is possible to conclude that most predicted values are very close to what was expected from the personality questionnaires, with the exception of the Neuroticism model. Using only features from the BVP signal, the models for Agreeableness, Extraversion and Openness to Experience are the ones that perform best and the worst performance belongs to the Neuroticism scale.

In Table 5.6 are presented the results of the evaluation of the model performance for each scale. Through this table, it is possible to see that all scales need less than 30 features to minimize the model error, with the Maximization scale needing only 25. With a prediction error of only 0.03, the scale with the best result is the Extraversion dimension of the FFM and the Openness to Experience scale has the second best result with 0.05. Three models, Conscientiousness, Neuroticism and Regret, have a prediction error equal to or greater than 0.1.

As expected, the Extraversion and Agreeableness models have the lowest model errors and Regret the highest. The Openness to Experience scale, despite presenting a prediction error of only 0.05, has the second highest model error due to not only the prediction error, but also the bias of the data and the error rrelated to the slope of the linear regression. The highest model error belongs to the Neuroticism scale as was expected due to the difference between the predicted and observed values visible in Figure 5.14d. In its majority, the results confirm the prior expectations obtained from the visualization of the Figures 5.13 and 5.14.

Also in Table 5.6, the best five features of each model are presented with 29 from 35 of them being different from each other, which makes possible to conclude that each scale is based on specific features. The most chosen features, *tt - mean BVP*, *b2 - mean BVP*, *b3 - maximum IBI*, *b5 - SD IBI*, *b3 - minimum IBI* and *tt - maximum pulse width*, were selected twice. Three out of the best five features from the Agreeableness predictive model are from Block 2 and also three of them are statistical features computed from IBI. From the five best features, the Regret model has four features which are statistical parameters extracted from the pulse width. The statistical features of IBI are equivalent to the statistical features extracted from the HRV signal, that was computed from the ECG signal, and are present ten times in the thirty-five best features from all models. However, the statistical features from *BAV*, *BVP* and *pulse width*, that depend directly of the BVP signal, represent 22 out of the 35 best features of all models. These features are directly correlated with vessel dilation/constriction, which are induced by sympathetic and parasympathetic activity, and are represented in all personality scales. It can be concluded that the use of features computed from BVP, that are not connected to HRV, is encouraged and the BVP signal should not be used only as a tool to extract HRV.

In Table 5.7, the number of features from the BVP signal selected by the classifier, from each block and from the complete task, are represented. For the Openness to Experience

Table 5.6: Results of the performance of the predictive model with BVP features: for each scale is presented the number of features used by the classifier, the best five features of each model, the model error and the mean error of the absolute differences between the predicted and the observed values.

Scale	Number of features	Best five features	Model Error	Prediction Error
O	26	*tt - mean BVP, b4 - SD IBI, b2 - SD BAV, b2 - SD pulse width, b5 - mean BVP*	1.07	0.05 ± 0.04
C	26	*b2 - mean BVP, b1 - SD BAV, b1 - BVP range, tt - mean BVP, b3 - max IBI*	0.92	0.1 ± 0.2
E	26	*b3 - mean BVP, tt - maximum peak time, b5 - minimum BAV, b2 - mean BVP, b5 - SD IBI*	0.48	0.03 ± 0.04
A	27	*b2 - maximum pulse width, b2 - minimum BAV, b3 - maximum IBI, b2 - SD IBI, b1 - SD IBI*	0.54	0.09 ± 0.08
N	28	*b5 - maximum pulse width, tt - maximum BVP, b3 - minimum IBI, b5 - minimum IBI, tt - SD BVP*	1.73	0.3 ± 0.8
Max	25	*b4 - SD pulse width, tt - maximum pulse width, b2 - BVP range, b3 - SD pulse width, b5 - SD IBI*	0.75	0.09 ± 0.09
R	26	*b4 - maximum pulse width, b3 - minimum IBI, tt - minimum pulse width, b3 - SD pulse width, tt - max pulse width*	1.29	0.2 ± 0.2

and Extraversion scales, most of the features were chosen from the entire task. The Conscientiousness predictive model has an equal number of features selected from the first, third and fourth blocks of the IGT. The Agreeableness scale has most features selected from Block 1 with the number of features from Block 2, Block 3 and the entire task coming in second. The Neuroticism scale predictive model has most features selected from Block 3 and the Maximization scale from Block 4. The Regret model has most features selected from Block 2. In general, the greatest number of features was selected fom the entire task using BVP features and the features from Block 5 were the least used.

Table 5.7: Number of features per block used by the classifier to predict each scale, with features extracted from BVP.

Scale	Complete	Block 1	Block 2	Block 3	Block 4	Block 5
O	6	4	5	3	4	4
C	4	5	4	5	5	3
E	7	4	3	4	2	6
A	5	7	5	5	4	1
N	6	2	6	7	4	3
Max	5	3	3	5	7	2
R	5	3	7	6	2	3
	38	28	33	35	28	22

5.3.4 Pupillometry Model

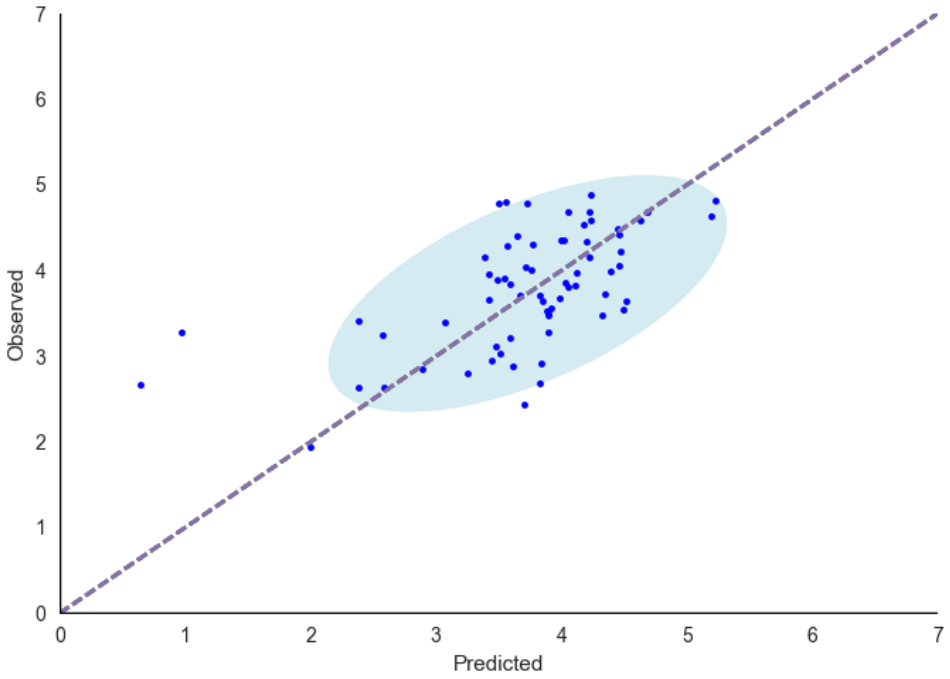

Figure 5.15: Predictive model result for the Conscientiousness scale, obtained with features from the pupillometry data.

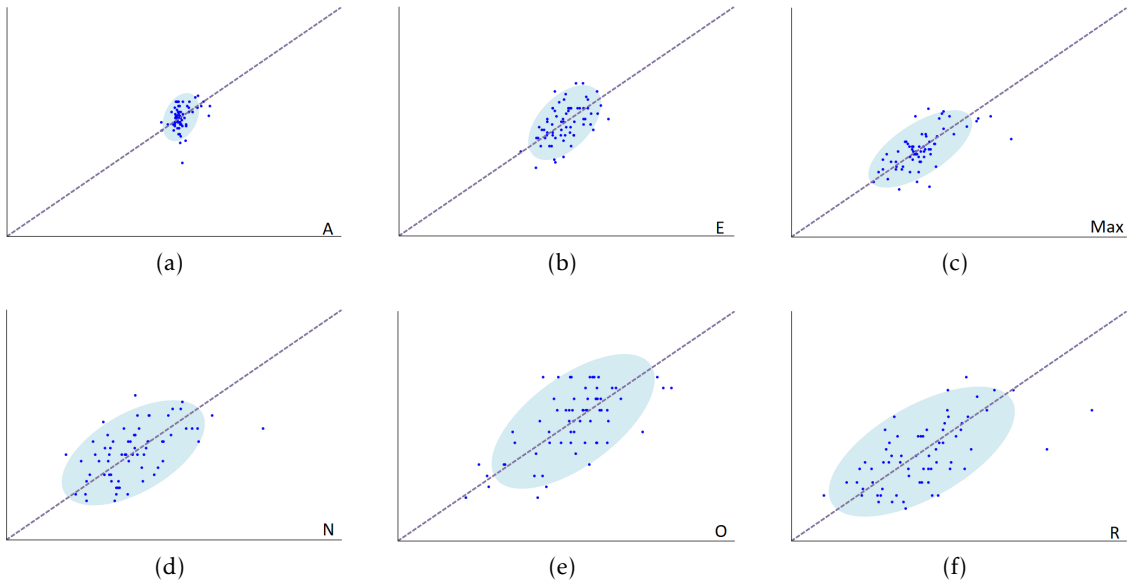

(a) (b) (c)

(d) (e) (f)

Figure 5.16: Predictive model results for Agreeableness (A), Extraversion (E), Maximization (Max), Neuroticism (N), Openness to Experience (O) and Regret (R), obtained with features from the pupillometry data.

The results retrieved from the best combination of features from the pupillometry signal for each personality scale are represented in the Figures 5.15 and 5.16, with the light blue ellipse representing the 95% confidence region of the data.

According to an initial visual inspection of the results, it is possible to conclude that a large part of the predicted values do not correspond to the real values, obtained by the personality questionnaires. Using only features from the pupillometry signal, the models for Agreeableness, Extraversion and Maximization are the ones which present the better results.

In Table 5.8 are presented the results of the evaluation of the model performance for each scale. Through this table, it is possible to see that all scales need less than 30 features to minimize the model error. With a prediction error of 0.3, the models with the best results correspond to the Agreeableness and the Maximization predictive models. All models have a prediction error equal or superior to 0.1, with the Regret model presenting the highest error of 0.7.

As expected, the Agreeableness model has the lowest model error and it is the only model that has a model error inferior to 1.

Also in Table 5.8, the best five features of each model are presented with 28 from 35 of them being different from each other.

The most chosen features, the *b2 - mean blink % in choice* and the *b2 - mean diameter variation in selection*, were selected three times. *b4 - SD blink % in feedback*, *b1 - SD diameter variation in choice* and *b5 - SD diameter variation in selection* were selected twice. From the five best features, the Conscientiousness model has four features which are extracted from the second Block. To improve the predictive models, other features should be implemented such as features that correlate events on the pupil diameter signal and the moments after a loss in IGT.

In Table 5.9, the number of features from the pupillometry signal selected by the classifier, from each block and from the complete task, are represented. The Openness to Experience model has most features selected from Block 1. The Conscientiousness predictive model has an equal number of features selected from the second and third blocks of the IGT. For the Extraversion and Maximization scales, most of the features were chosen from Block 2. The Agreeableness and Neuroticism predictive models have most features selected from Block 4. The Regret predictive model has an equal number of features selected from Block 1, 4 and 5. Globally, the greatest number of features was selected fom the Block 4 using only pupillometry features and the features from the entire task were the least used.

Table 5.8: Results of the performance of the predictive model with pupillometry features: for each scale is presented the number of features used by the classifier, the best five features of each model, the model error and the mean error of the absolute differences between the predicted and the observed values.

Scale	Number of features	Best five features	Model Error	Prediction Error
O	19	*b1 - peaks in selection, tt - mean AUC in choice, b1 - SD diameter variation in choice, b5 - SD diameter variation in selection, b5 - SD blink % in feedback*	1.85	0.6 ± 0.5
C	25	*b2 - mean blink % in choice, b2 - mean blink % in selection, b2 - mean diameter variation in choice, b3 - mean diameter variation in choice, b2 - SD diameter in selection*	1.40	0.5 ± 0.4
E	18	*b3 - mean blink % in feedback, b4 - SD blink % in feedback, b4 - SD diameter in selection, b2 - mean diameter variation in selection, b2 - mean blink % in choice*	1.07	0.4 ± 0.3
A	10	*b3 - mean diameter variation in feedback, b4 - peaks in feedback, b3 - SD blink % in feedback, b5 - mean blink % in selection, b4 - mean diameter variation in feedback*	0.74	0.3 ± 0.2
N	27	*b3 - SD blink % in selection, b4 - SD blink % in feedback, b1 - SD diameter variation in choice, b3 - mean blink % in choice, b1 - SD blink % in feedback*	1.55	0.6 ± 0.4
Max	15	*tt - SD diameter in selection, b2 - SD blink % in feedback, b4 - SD blink % in selection, b1 - SD diameter in selection, b2 - mean diameter variation in selection*	1.07	0.3 ± 0.3
R	26	*b5 - SD diameter variation in choice, b5 - SD diameter variation in selection, b2 - mean diameter variation in selection, b4 - mean diameter in choice, b2 - mean blink % in choice*	1.88	0.7 ± 0.5

Table 5.9: Number of features per block used by the classifier to predict each scale, with features extracted from pupillometry.

Scale	Complete	Block 1	Block 2	Block 3	Block 4	Block 5
O	2	6	1	4	2	4
C	2	1	6	6	5	5
E	3	0	5	2	4	4
A	0	2	0	2	5	1
N	3	3	4	7	8	2
Max	1	3	5	0	3	3
R	2	6	4	2	6	6
	13	21	25	23	33	25

5.3.5 Biosignals Model

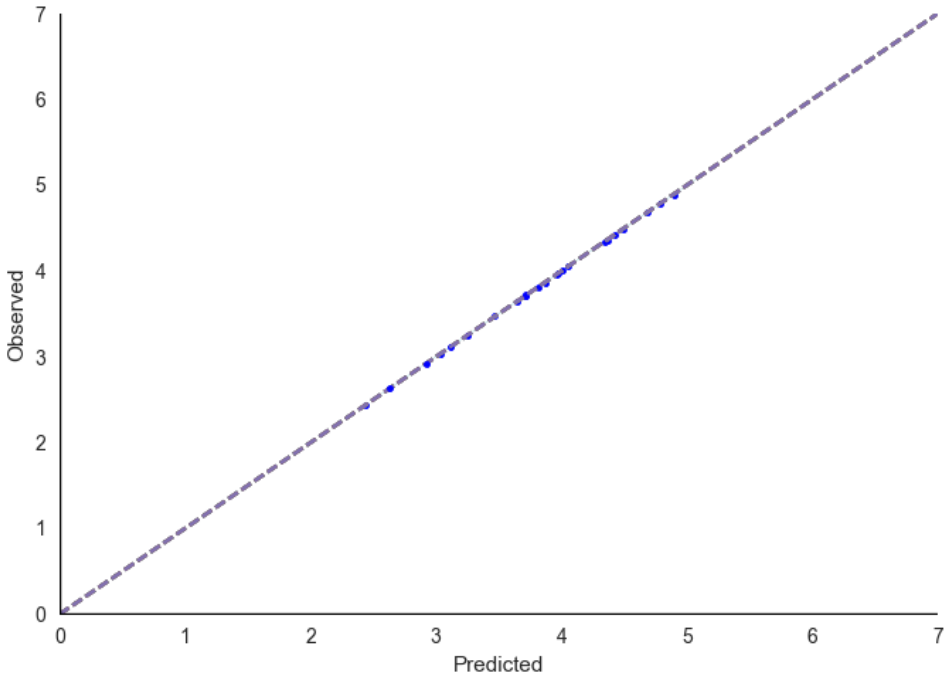

Figure 5.17: Predictive model result for the Conscientiousness scale, obtained with features from all biosignals used in this thesis.

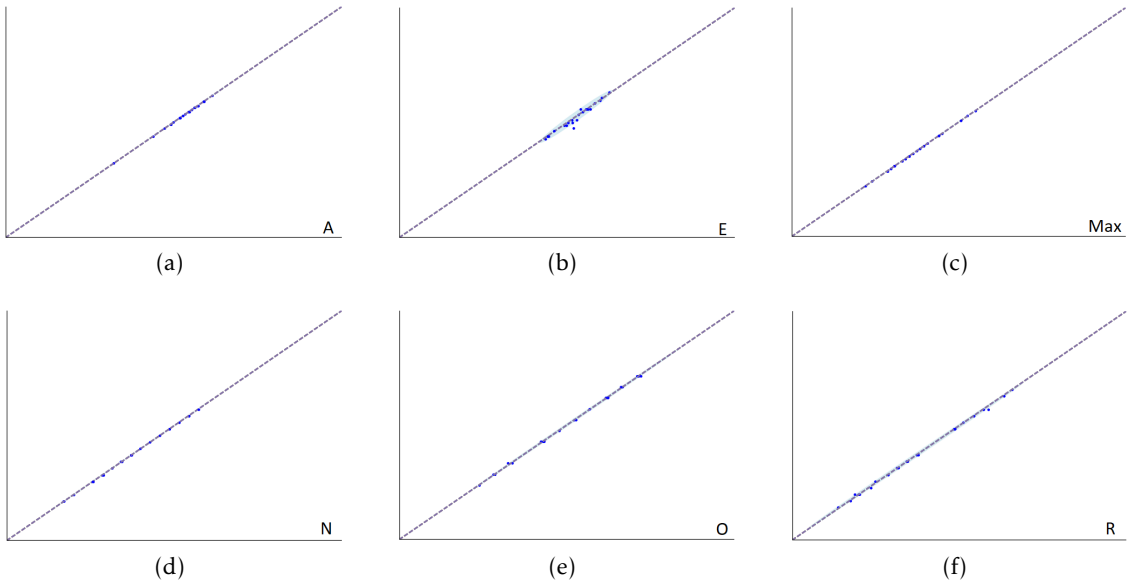

(a) (b) (c)

(d) (e) (f)

Figure 5.18: Predictive model results for Agreeableness (A), Extraversion (E), Maximization (Max), Neuroticism (N), Openness to Experience (O) and Regret (R), obtained with features from all biosignals.

In this section, the results obtained for the best combination of features from all biosignals for each personality scale are presented in the Figures 5.17 and 5.18, with the light blue ellipse representing the 95% confidence region of the data.

Through visual inspection of the results, it is visible that all predicted values are very close to what was expected from the questionnaire results. This means that the predictive models are classifying this thesis population correctly. Using features from all biosignals, the Extraversion and Regret models are the predictive models that should have the biggest prediction error.

In Table 5.10 are presented the results of the evaluation of the model performance for each scale. Through this table, it is possible to see that all scales need 20 or less features to minimize the model error, with the Regret scale needing only 17 features. All scales present optimal results, however the Conscientiousness, Agreeableness, Neuroticism and Maximization models have a prediction error inferior to 0.01, while the Openness to Experience and Regret scales have an error of 0.02 and the Extraversion an error of 0.05. The Openness to Experience and Regret models are the only scales that have a intrinsic model error superior to 1. These results verify the initial expectations obtained from the visualization of Figures 5.17 and 5.18.

Also in Table 5.10, the best five features of each model are presented with 33 from 35 of them being different from each other, which makes possible to conclude that each scale is based on very specific features.

The *b1 - maximum SCR rise time* was the most chosen feature, being present in Neuroticism (2nd best), Maximization (3rd best) and Regret scales (2nd best). Notably, thirteen features from Block 1 were chosen, so this block is the most represented in best fives features of all prediction models. Also, three out of the best four features of the Maximization model are from Block 1. The features from the entire task and the features from the last block were only chosen 3 times each.

Statistical features from the *SCR rise time* and the *BVP pulse width* were selected three times across all predictive models, with the *HRV triangular index*, *HRV HF*, *HRV TINN*, *SCR amplitude*, *SD diameter in choice* and *SCR in selection* being chosen twice. The Openness to Experience model best four features are extracted from the ECG signal and, from this four, three are geometrical features extracted from the HRV, the TINN and HRV triangular index. These features are related to overall changes in the HRV signal, but are more influenced by low frequencies. Since the low frequencies are associated with the balance between SNS and PSNS, changes in both branches of the ANS during the performance of the IGT my be related to the Openness to Experience dimension of the FFM.

For the Openness to Experience and Extraversion models, four out of the five best features was extracted from the ECG signal and the remaining feature came from the pupillometry data. The Maximization scale predictive model is the only model that has features extracted from all biosignals in its five best features. The Agreeableness and

Table 5.10: Results of the performance of the predictive model with all biosignals: for each scale is presented the number of features used by the classifier, the best five features of each model, the model error and the mean error of the absolute differences between the predicted and the observed values.

Scale	Number of features	Best five features	Model Error	Prediction Error
O	18	*b2 - HRV triangular index, b1 - HF, b5 - TINN, tt - TINN, b1 - mean diameter variation in selection*	1.12	0.02 ± 0.02
C	19	*b4 - total power, b1 - minimum SCR amplitude, b2 - HF, b2 - SD diameter in choice, b3 - SD SCL*	0.66	0.002 ± 0.002
E	20	*b4 - SD diameter in choice, b1 - % VLF, b4 - LF/HF, b1 - HF peak, b5 - FD*	0.48	0.05 ± 0.07
A	19	*b3 - LF, b4 - minimum SCR amplitude, b2 - SD IBI, b1 - SD BAV, b1 - mean SCR peak rate*	0.44	0.004 ± 0.004
N	19	*b5 - SCR in selection, b1 - maximum SCR rise time, tt - minimum pulse width, b1 - SD1/SD2, b3 - minimum pulse width*	0.82	0.005 ± 0.005
Max	20	*b1 - CD, b3 - SD AUC in selection, b1 - maximum SCR rise time, b1 - % HF, tt - maximum pulse width*	0.59	0.003 ± 0.002
R	17	*b4 - SCR in selection, b1 - maximum SCR rise time, b3 - stress index, b4 - SCR in choice, b3 - HRV triangular index*	1.14	0.02 ± 0.03

Neuroticism models have features extracted from ECG, EDA and BVP, while the Conscientiousness predictive model selected features from ECG, EDA and pupillometry data. The Regret model has only ECG and EDA features on its five best features that minimize the prediction error. With these results, it is possible to conclude that different biosignals are useful to extract different information in order to obtain better performances on the personality predictive models and their combined use is encouraged to achieve better results using less features than the models which rely on only one biosignal.

In Table 5.11, the number of features selected by the classifier, from each block and from the complete task, are represented. As can be seen in this table, the total number of features extracted from all blocks and from the entire task, except for the first block, is inferior to 20 with the first block standing out from the others with 62 features present in

the best models of all personality scales. All models had most features selected from the first block as well. One more time, the hypothesis that personality traits are more evident in the beginning of the decision-making task is comproved.

Table 5.11: Number of features per block used by the classifier to predict each scale, with features from all biosignals.

Scale	Complete	Block 1	Block 2	Block 3	Block 4	Block 5
O	4	10	1	0	2	1
C	3	11	2	1	1	1
E	2	9	2	0	4	3
A	2	8	2	3	1	3
N	1	6	5	2	2	3
Max	2	11	4	1	1	1
R	1	7	3	4	2	0
	15	62	19	11	13	12

In Table 5.12, it is represented the number of features extracted from each biosignal used by the classifer to predict all personality scales. As can be seen, most features are selected from the ECG and EDA signals, which are the most chosen for the Conscientiousness, Extraversion, Agreeableness and Regret predictive models. The Neuroticism and Maximization scales have most features extracted from the BVP and EDA. Features from ECG are the most chosen for the Openness to Experience, Conscientiousness, Extraversion and Regret models. The Agreeableness predictive model has most features obtained through the EDA signal, while BVP had the highest number of selected features in the Neuroticism and Maximization models. All predictive models use at least one feature from each biosignal. Once again the importance of using several biosignals to minimize the prediction error and the number of used features is verified.

Table 5.12: Number of features per biosignal used by the classifier to predict each personality scale.

Scale	Number of features	ECG	EDA	BVP	Pupillometry
O	18	10	2	3	3
C	19	7	6	1	5
E	20	7	5	4	4
A	19	5	9	2	3
N	19	4	5	6	4
Max	20	4	6	7	3
R	17	8	5	2	2
		45	38	25	24

5.3.6 General Discussion

In this last section of the analysis of the predictive models, the results obtained for each biosignal and for the combination of all of them are compared in order to reach some conclusions.

The Openness to Experience scale is well predicted using only features from the ECG and from BVP, with the first scoring the lowest prediction error of 0.01. On the other hand, the Agreeableness and Maximization scales best results came from using features from the ECG and EDA biosignals and in both cases the models that worked with ECG features had the lowest prediction errors. The Extraversion predictive models using EDA and BVP produced good results, with the latter having the lowest prediction error, 0.03.

The predictive models based on ECG features present slightly better results, using less features, in comparison with the EDA based models, which have bigger prediction errors and use more features to minimize the error of the model. The BVP models for Extraversion and Openness to Experience scales show prediction errors results of the order of magnitude of the ECG and EDA results but with almost less 20 features used to make the prediction. These results encourage the conclusion that more BVP features should be used to decrease the number of features selected by the models to minimize the errors of prediction.

The ECG and BVP models both use statistical features computed from the HRV signal. All ECG based models did not have statistical HRV features selected in the best five features of the model, in contrast to the BVP based models.

The predictive models based on features extracted from the pupillometry data present the worst results of all predictive models. To improve these models, the introduction of features that correlate the pupil diameter signal with the events occuring in the IGT should be tested since pupil activity is connected with ANS activity.

In order to confirm the hypothesis that the personality traits are more expressed in the beginnig of the IGT, when people are unaware of the best strategy to use in order to win the game, the number of features from each block for all the models was counted. The predictive models using ECG and EDA and the models computed with the features from all studied biosignals confirm this hypothesis with the features from the Block 1 being the most chosen by the models.

Considering only the best five features of each model, the Openness to Experience scale has most features selected from Block 1 for the models that use features from ECG, EDA, pupillometry and all biosignals. The Agreeableness predictive models best five features are most chosen from Block 1 in the EDA, BVP and all biosignals based models. In the Neuroticism scale this happens for the models that use features from ECG, EDA and all biosignals. So, it is possible to assume that these three personality dimensions are more expressed in the first instants of the IGT.

According to the model errors from the models with ECG, EDA, BVP and pupillometry features, the Openness to Experience, Agreeableness and Maximization scales have the

lowest model error using features from ECG, the Conscientiousness, Neuroticism and Regret using features from EDA and the Extraversion using features from BVP. The Openness to Experience, Agreeableness and Regret best predictive models using only features from one biosignal present lower model errors than the respective predictive models computed from features from all biosignals.

The predictive models that use features from all biosignals presented optimal results for all tested personality scales. In these models, features from ECG, EDA, BVP and pupillometry data are used. This fact reinforces the conclusion that features from the several biosignals should be used to predict personlity since these results present the lowest prediction error of all tested models and also use the lowest number of features to predict.

The best five features of the models based on all biosignals were compared with the best five from each individual biosignal model. The *b2 - SD IBI* feature was selected, as one of the best five features, for the BVP Agreeableness model as well as for the model with all biosignals. The *b5 - SCR in selection* feature was also selected for the EDA Neuroticism model as well as for the model with all biosignals. And also, the *tt - maximum pulse width* feature was selected, as one of the best five features, for the BVP model for the Maximization scale, as well as for the model with all biosignals. To conclude, the best five features of the models in which an unique biosignal was used, usually, were not also chosen as best features by the model with features from all signals. This fact is explained by the feature selection method, since the second, third, fourth, ..., best features are selected to minimize the error of their combination with the previous chosen features. Due to this, it is possible that the features selected from the biosignals model do not correspond with the features selected by the models that use only one biosignal.

Chapter 6

Conclusions

In the last chapter of this thesis, the work that was developed is summarized as well as the most important results. Some suggestions of feature work are also given.

6.1 General Results

The main objective of this dissertation was the construction of predictive models of personality based on features extracted from biosignals during the performance of a gambling task.

To do this, the BVP, EDA, ECG and pupillometry biosignals, acquired during the realization of the IGT, were processed in order to proceed with the extraction of meaningful features of each signal. All processing tools proved to be effective for the extraction of features.

A secondary aim of this thesis was to implement and validate the EDA processing model proposed by Gamboa [38]. Alterations made to the filtering step reduced the time required to extract features and also improved the peak detection. The efficiency of this model to detect low amplitude events and overlapping events was comproved.

During the realization of this thesis, another objective emerged: finding features that could correlate events happening on IGT with the EDA signal. To do this, the losses on IGT were correlated with the events occuring in the EDA signal and results that were obtained comprove that there is a relationship between losses on IGT and arousal detected through the EDA signal.

After concluding the feature extraction from all biosignals, the predictive models were computed according to a machine learning algorithm that selects the best combination of features that minimizes the model error. In summary, the Openness to Experience, Agreeableness and Maximization scales are well predicted with ECG features, especially

features related to the low frequencies of the HRV which is thought to be related to the balance between the SNS and the SNS. So, these personality scales can be related to changes in the ANS activity. The Extraversion, Agreeableness and Maximization scales present low prediction errors in the models computed from the EDA features. Since the events in EDA are related to SNS activation, sympathetic activity triggered by the performance of the IGT can be related to these personality scales. The Openness to Experience and Extraversion scales are well predicted with statistical features from BVP and BAV, which are related with ANS activity. So, it is possible that the changes in ANS are related to these personality scales. The Neuroticism, Conscientiousness and Regret models, in general, have the highest prediction errors among all models. It is possible that these scales do not have a direct correlation with ANS activity. From these results, the models that use ECG features present the lowest prediction errors. The worst results of all predictive models belong to the pupillometry features based model. The highest number of features is extracted from the IGT Block 1 which can be explained by our hypothesis that personality traits are more expressed in the beginnig of the IGT, when people are unaware of the best strategy to use in order to win the game.

The Conscientiousness, Extraversion, Neuroticism and Maximization models with the lowest model errors are computed with features from all the biosignals, while the Openness to Experience and Agreeableness models are computed from ECG features and the Regret model from EDA features. Globally, the predictive models with features from all biosignals present the best results of all tested models and should be further used to achieve better the results.

6.2 Future Work

To conclude the development of this thesis, some topics of improvements are introduced to future researches.

All predictive models could be improved with the introduction of features that correlate events on IGT and events on the physiological signals. Since the 'Correlation with loss' features from the EDA signal proved to be effective for predicting personality, new features that correlate EDA with IGT features should be implemented in order to reduce the number of features required. For example, features that correlate the anticipatory moments of a decision on IGT with the events on EDA should be tested since the physiological responses when choosing a risky or a non risky deck could be different.

The introduction of other biosignals, such as respiration, could improve the models accuracy. The development of new features extracted from the pupillometry data could also improve these models results.

The validation of these results should also be extended to other subjects, so the models could be validated with different populations to verify if their accuracy remains unchanged. This validation could be important to solidify the results that showed that personality can be identified through electrophysiological behavior.

The results should also be applied and tested in real-life decision making situations, such as the hospital environment.

Bibliography

[1] H. A. Simon. "A Behavioral Model of Rational Choice". In: *The Quarterly Journal of Economics* 69.1 (1955), pp. 99–118.

[2] M. Annett. "A classification of hand preference by association analysis". In: *Br. J. Psychol.* 61.3 (1970), pp. 303–321.

[3] B. G. Wallin. "Sympathetic nerve activity underlying electrodermal and cardiovascular reactions in man". In: *Psychophysiology* 18.4 (1981), pp. 470–476.

[4] J. Pan and W. Tompkins. "A Real-Time QRS Detection Algorithm". In: *IEEE Transactions on Biomedical Engineering* 32.3 (1985), pp. 230–236.

[5] J. D. Bronzino. *Biomedical engineering and instrumentation: basic concepts and applications*. PWS Engineering, 1986.

[6] P. T. Costa and R. R. McCrae. "Four ways five factors are basic". In: *Personality and Individual Differences* 13.6 (1992), pp. 653–665.

[7] R. R. McCrae and O. P. John. "An introduction to the five-factor model and its applications." In: *Journal of Personality* 60.2 (1992), pp. 175–215.

[8] P. Borkenau and F. Ostendorf. *NEO-Fünf-Faktoren-Inventar (NEO-FFI) nach Costa und McCrae*. Göttingen: Hogrefe, 1993, pp. 5–10, 27–28.

[9] A. Bechara, A. Damasio, H. Damasio, and S. Anderson. "Insensitivity to future consequences following damage to human prefrontal cortex". In: *Cognition* 50 (1994), pp. 7–15.

[10] L. W. Freedman, A. S. Scerbo, M. E. Dawson, A. Raine, W. O. Mcclure, and P. H. Venables. "The relationship of sweat gland count to electrodermal activity". In: *Psychophysiology* 31.2 (1994), pp. 196–200.

[11] J. Hyona, J. Tommola, and A. Alaja. "Pupil dilation as a measure of processing load in simultaneous interpretation and other language tasks". In: *The Quarterly Journal of Experimental Psychology* 48A.3 (1995), pp. 598–612.

[12] M. Malik, T. J. Bigger, A. J. Camm, R. E. Kleiger, A. Malliani, A. J. Moss, and J. P. Schwartz. "Heart rate variability Standards of measurement, physiological interpretation, and clinical use". In: *European Heart Journal* 17 (1996), pp. 354–381.

[13] C. L. Lim, C. Rennie, R. J. Barry, H. Bahramali, I. Lazzaro, B. Manor, and E. Gordon. "Decomposing skin conductance into tonic and phasic components". In: *International Journal of Psychophysiology* 25 (1997), pp. 97–109.

[14] M. P. de Lima. "NEO-PI-R Contextos teóricos e psicométricos "OCEAN"ou "iceberg"?" PhD thesis. Universidade de Coimbra, 1997.

[15] R. D. Rogers, A. M. Owen, H. C. Middleton, E. J. Williams, J. D. Pickard, B. J. Sahakian, and T. W. Robbins. "Choosing between Small , Likely Rewards and Large , Unlikely Rewards Activates Inferior and Orbital Prefrontal Cortex". In: 20.19 (1999), pp. 9029–9038.

[16] J. Enderle, S. Blanchard, and J. Bronzino. *Introduction to Biomedical Engineering*. Academic Press, 2000.

[17] B. Schwartz. "Self-determination: The tyranny of freedom." In: *American Psychologist* 55.1 (2000), pp. 79–88.

[18] J. Dempster. *The Laboratory Computer: A Practical Guide for Physiologists and Neuroscientists*. Academic Press, 2001, p. 233.

[19] L Hejjel and I Gál. "Heart rate variability analysis". In: *Acta Physiologica Hungarica* 88 (2001), pp. 219–230.

[20] N. Schmitz, N. Hartkamp, C. Baldini, J. Rollnik, and W. Tress. "Psychometric properties of the German version of the NEO-FFI in psychosomatic outpatients". In: *Personality and Individual Differences* 31 (2001), pp. 713–722.

[21] H. D. Critchley. "Electrodermal responses: what happens in the brain." In: *The Neuroscientist* 8.2 (2002), pp. 132–142.

[22] B. Schwartz, A. Ward, J. Monterosso, S. Lyubomirsky, K. White, and D. R. Lehman. "Maximizing versus satisficing: happiness is a matter of choice". In: *Journal of Personality and Social Psychology* 83.5 (2002), pp. 1178–1197.

[23] M. Hansenne. *Psicologia da personalidade*. 1ª edição. Lisboa: Climepsi Editores, 2003.

[24] T. Partala and V. Surakka. "Pupil size variation as an indication of affective processing". In: *International Journal of Human Computer Studies* 59 (2003), pp. 185–198.

[25] W. Zong, T. Heldt, G. B. Moody, and R. G. Mark. "An Open-Source Algorithm to Detect Onset of Arterial Blood Pressure Pulses". In: *Computers in Cardiology* 30 (2003), pp. 259–262.

[26] E. A. Crone, R. J. M. Somsen, B. V. Beek, and M. W. V. Der Molen. "Heart rate and skin conductance analysis of antecendents and consequences of decision making". In: *Psychophysiology* 41 (2004), pp. 531–540.

[27] R. R. McCrae and P. T. Costa Jr. "A contemplated revision of the NEO Five-Factor Inventory". In: *Personality and Individual Differences* 36 (2004), pp. 587–596.

[28] L. Sherwood. *Human Physiology - From Cells to Systems*. 5th Ed. Thomson Learning, Inc., 2004, pp. 133–136,237–242.

[29] U. R. Acharya, K. P. Joseph, N Kannathal, C. M. Lim, and J. S. Suri. "Heart rate variability: A review". In: *Medical and Biological Engineering and Computing* 44.12 (2006), pp. 1031–1051.

[30] R. Dorf. *The Biomedical Engineering Handbook*. Ed. by J. D. Bronzino. 3rd Ed. CRC Press, 2006.

[31] A. E. Goudriaan, J. Oosterlaan, E. de Beurs, and W. van den Brink. "Psychophysiological determinants and concomitants of deficient decision making in pathological gamblers". In: *Drug and Alcohol Dependence* 84 (2006), pp. 231–239.

[32] R. Greifeneder and C. Betsch. "Lieber die Taube auf dem Dach! Eine Skala zur Erfassung interindividueller Unterschiede in der Maximierungstendenz". In: *Zeitschrift für Sozialpsychologie* 37.4 (2006), pp. 233–243.

[33] S. M. Kuo, B. H. Lee, and W. Tian. *Real-Time Digital Signal Processing: Implementations and Applications*. 2nd Ed. John Wiley & Sons Ltd, 2006, pp. 3–6.

[34] A. T. Reisner, G. D. Clifford, and R. G. Mark. "The Physiological Basis of the Electrocardiogram". In: *Advanced methods and tools for ECG data analysis*. 2006. Chap. 1, pp. 1–25.

[35] B. W. Balleine. "The Neural Basis of Choice and Decision Making". In: *Journal of Neuroscience* 27.31 (2007), pp. 8159–8160.

[36] M. Brand, E. C. Recknor, F. Grabenhorst, and A. Bechara. "Decisions under ambiguity and decisions under risk : Correlations with executive functions and comparisons of two different gambling tasks with implicit and explicit rules". In: *Journal of Clinical and Experimental Neuropsychology* 29.1 (2007), pp. 86–99.

[37] J. Cacioppo, L. G. Tassinary, and G. G. Berntson. *Handbook of Psychophysiology*. 2007.

[38] H. F. S. Gamboa and A. L. N. Fred. "An Electrodermal Activity Psychophysiologic Model". In: *The International Educational and Networking Forum for eHealth, Telemedicine and Health ICT*. 2007, pp. 88–81.

[39] J. D. Hunter. "Matplotlib: A 2D Graphics Environment". In: *Computing in Science & Engineering* 9 (2007), pp. 90–95.

[40] D. Lee, M. F. S. Rushworth, M. E. Walton, M. Watanabe, and M. Sakagami. "Functional specialization of the primate frontal cortex during decision making". In: *The Journal of Neuroscience* 27.31 (2007), pp. 8170–8173.

[41] E. A. Murray, J. P. O'Doherty, and G. Schoenbaum. "What We Know and Do Not Know about the Functions of the Orbitofrontal Cortex after 20 Years of Cross-Species Studies". In: *Journal of Neuroscience* 27.31 (2007), pp. 8166–8169.

[42] E. Peper, R. Harvey, I.-M. Lin, H. Tylova, and D. Moss. "Is There More to Blood Volume Pulse Than Heart Rate Variability , Respiratory Sinus Arrhythmia , and Cardiorespiratory Synchrony ?" In: *Biofeedback* 35.2 (2007), pp. 54–61.

[43] L. Salahuddin, J. Cho, M. G. Jeong, and D. Kim. "Ultra Short Term Analysis of Heart Rate Variability for Monitoring Mental Stress in Mobile Settings". In: *IEEE Engineering in Medicine and Biology Society*. 2007, pp. 4656–4659.

[44] B. M. Asl, S. K. Setarehdan, and M. Mohebbi. "Support vector machine-based arrhythmia classification using reduced features of heart rate variability signal". In: *Artificial Intelligence in Medicine* 44 (2008), pp. 51–64.

[45] M. M. Bradley, L. Miccoli, M. A. Escrig, and P. J. Lang. "The pupil as a measure of emotional arousal and autonomic activation". In: *Psychophysiology* 45 (2008), pp. 602–607.

[46] W. Einhäuser, J. Stout, C. Koch, and O. Carter. "Pupil dilation reflects perceptual selection and predicts subsequent stability in perceptual rivalry". In: *Proceedings of the National Academy of Sciences*. Vol. 105. 5. 2008, pp. 1704–1709.

[47] S. Moresi, J. J. Adam, J. Rijcken, P. W.M. V. Gerven, H. Kuipers, and J. Jolles. "Pupil dilation in response preparation". In: *International Journal of Psychophysiology* 67 (2008), pp. 124–130.

[48] R. Orsila, M. Virtanen, T. Luukkaala, M. Tarvainen, J. Viik, M. Savinainen, and C.-H. Nygård. "Perceived Mental Stress and Reactions in Heart Rate Variability — A Pilot Study Among Employees of an Electronics Company". In: *International Journal of Occupational Safety and Ergonomics* 14.3 (2008), pp. 275–283.

[49] G. Piñeiro, S. Perelman, J. P. Guerschman, and J. M. Paruelo. "How to evaluate models : Observed vs. predicted or predicted vs. observed ?" In: *Ecological Modelling* 216 (2008), pp. 316–322.

[50] D. R. Bach, G. Flandin, K. J. Friston, and R. J. Dolan. "Time-series analysis for rapid event-related skin conductance responses". In: *Journal of Neuroscience Methods* 184 (2009), pp. 224–234.

[51] A. Dix. "Human-Computer Interaction". In: *Encyclopedia of Database Systems*. Boston, MA: Springer US, 2009, pp. 1327–1331.

[52] J.-M. Hupé, C. Lamirel, and J. Lorenceau. "Pupil dynamics during bistable motion perception". In: *Journal of Vision* 9.7 (2009), pp. 1–19.

[53] A. Kampouraki, G. Manis, and C. Nikou. "Heartbeat Time Series Classification-With Support Vector Machines". In: *IEEE Transactions on Information Technology in Biomedicine*. Vol. 13. 4. 2009, pp. 512–518.

[54] M. Benedek and C. Kaernbach. "A continuous measure of phasic electrodermal activity". In: *Journal of Neuroscience Methods* 190 (2010), pp. 80–91.

[55] W. Einhäuser, C. Koch, and O. L. Carter. "Pupil dilation betrays the timing of decisions". In: *Frontiers in Human Neuroscience* 4 (2010), pp. 1–9.

[56] W. McKinney. "Data Structures for Statistical Computing in Python". In: *Proceedings of the 9th Python in Science Conference*. 2010, pp. 51–56.

[57] J. Medeiros, R. Martins, S. Palma, H. Gamboa, and M. Reis. "Blood Volume Pulse Peak Detector with a Double Adaptive Threshold". In: *Proc. of TMSi*. 2010.

[58] A. Pantelopoulos and N. G. Bourbakis. "A Survey on Wearable Sensor-Based Systems for Health Monitoring and Prognosis". In: *IEEE Transactions on Systems, Man, and Cybernetics - Part C: Applications and reviews* 40.1 (2010), pp. 1–12.

[59] C. Setz, B. Arnrich, J. Schumm, R. L. Marca, G. Troster, and U. Ehlert. "Discriminating Stress From Cognitive Load Using a Wearable EDA Device". In: *IEEE Transactions on Information in Biomedicine*. Vol. 14. 2. 2010, pp. 410–417.

[60] F. S. Bao, X. Liu, and C. Zhang. "PyEEG : An Open Source Python Module for EEG / MEG Feature Extraction". In: *Computational Intelligence and Neuroscience* (2011).

[61] L. J. Drucaroff, R. Kievit, S. M. Guinjoan, E. Roldán Gerschcovich, D. Cerquetti, R. Leiguarda, D. P. Cardinali, and D. E. Vigo. "Higher Autonomic Activation Predicts Better Performance in Iowa Gambling Task". In: *Cognitive and behavioral neurology* 24 (2011), pp. 93–98.

[62] D. Jenkins and S. Gerred. *ECGs by Example*. 3rd Ed. Elsevier, 2011.

[63] A. Kushki, J. Fairley, S. Merja, G. King, and T. Chau. "Comparison of blood volume pulse and skin conductance responses to mental and affective stimuli at different anatomical sites". In: *Physiological Measurement* 32.10 (2011), pp. 1529–1539.

[64] K. J. Millman and M. Aivazis. "Python for Scientists and Engineers". In: *Computing in Science & Engineering* 13 (2011), pp. 9–12.

[65] F. Pedregosa, R. Weiss, and M. Brucher. "Scikit-learn : Machine Learning in Python". In: *Journal of Machine Learning Research* 12 (2011), pp. 2825–2830.

[66] S. van der Walt, S. C. Colbert, and G. Varoquaux. "The NumPy Array: A Structure for Efficient Numerical Computation". In: *Computing in Science & Engineering* 13 (2011), pp. 22–30.

[67] M. Elgendi. "On the Analysis of Fingertip Photoplethysmogram Signals". In: *Current Cardiology Reviews* 8 (2012), pp. 14–25.

[68] E. Kaniusas. "Fundamentals of Biosignals". In: *Biomedical Signals and Sensors I*. 2012. Chap. 1, pp. 1–21.

[69] M. M. Mukaka. "Statistics Corner : A guide to appropriate use of Correlation coefficient in medical research". In: *Malawi Medical Journal* 24.3 (2012), pp. 69–71.

[70] H. Silva, A. Fred, and A. Lourenço. "Electrodermal Response Propagation Time as a Potential Psychophysiological Marker". In: *IEEE Engineering in Medicine and Biology Society*. 2012, pp. 6756–6759.

[71] K. Starcke and M. Brand. "Decision making under stress: A selective review". In: *Neuroscience and Biobehavioral Reviews* 36 (2012), pp. 1228–1248.

[72] S. M. Wierda, H. van Rijn, N. A. Taatgen, and S. Martens. "Pupil dilation deconvolution reveals the dynamics of attention at high temporal resolution". In: *Proceedings of the National Academy of Sciences* 109.22 (2012), pp. 8456–8460.

[73] E. Bressert. *SciPy and NumPy*. O'Reilly Media, 2013.

[74] C. Kappeler-Setz, F. Gravenhorst, J. Schumm, B. Arnich, and G. Tröster. "Towards long term monitoring of electrodermal activity in daily life". In: *Pers Ubiquit Comput* 17 (2013), pp. 261–271.

[75] A. Paula and C. Figueira. "O Iowa Gambling Task : Uma Revis{ã}o Cr{í}tica The Iowa Gambling Task : A Critical Revision". In: 29.1994 (2013), pp. 201–210.

[76] V. Alexandratos, M. Bulut, and R. Jasinschi. "Mobile Real-Time Arousal Detection". In: *IEEE International Conference on Acoustic, Speech and Signal Processing*. 2014, pp. 4427–4431.

[77] J. W. de Gee, T. Knapen, and T. H. Donner. "Decision-related pupil dilation reflects upcoming choice and individual bias". In: *Proceedings of the National Academy of Sciences*. 2014, pp. 618–625.

[78] W. Handouzi, C. Maaoui, A. Pruski, and A. Moussaoui. "Objective model assessment for short-term anxiety recognition from blood volume pulse signal". In: *Biomedical Signal Processing and Control* 14 (2014), pp. 217–227.

[79] C. Lavín, R. S. Martín, and E. R. Jubal. "Pupil dilation signals uncertainty and surprise in a learning gambling task". In: *Frontiers in Behavioral Neuroscience* 7 (2014), pp. 1–8.

[80] S. A. Lowe and G. ÓLaighin. "Monitoring human health behaviour in one's living environment: A technological review". In: *Medical Engineering and Physics* 36 (2014), pp. 147–168.

[81] E. Magalhães, A. Salgueira, A.-J. Gonzalez, J. J. Costa, M. J. Costa, P. Costa, and M. P. de Lima. "NEO-FFI: Psychometric Properties of a Short Personality Inventory in Portuguese Context". In: *Psicologia: Reflexão e Crítica* 27.4 (2014), pp. 642–657.

[82] X. Wang, Y. Gu, Z. Xiong, Z. Cui, and T. Zhang. "Silk-Molded Flexible, Ultrasensitive, and Highly Stable Electronic Skin for Monitoring Human Physiological Signals". In: *Advanced Materials* 26 (2014), pp. 1336–1342.

[83] B. Koichubekov, I. Korshukov, N. Omarbekova, V. Riklefs, M. Sorokina, and X. Mkhitaryan. "Computation of nonlinear parameters of heart rhythm using short time ECG segments". In: *Computational and Mathematical Methods in Medicine* (2015).

[84] D. Shepherd, J. Mulgrew, and M. J. Hautus. "Autonomic Neuroscience : Basic and Clinical Exploring the autonomic correlates of personality". In: *Autonomic Neuroscience: Basic and Clinical* (2015).

[85] A. G.C. B. da Silva, D. N. Araujo, A. C. M. Costa, B. A. L. Dias, G. A.d. F. Fregonezi, and F. A. L. Dias. "Increase in perceived stress is correlated to lower heart rate variability in healthy young subjects". In: *Acta Scientiarum* 37.1 (2015), pp. 7–10.

[86] K. Gok and N. Atsan. "Decision-Making under Stress and Its Implications for Managerial Decision-Making: A Review of Literature". In: 06.03 (2016), pp. 38–47.

[87] Z. Liza and E. Eitan. "Contributions of Personality Dimensions to Spontaneous and Deliberate Information Processing in the Guilty Actions Test". In: *International Journal of Psychophysiology* (2016).

[88] R. Subramanian, J. Wache, M. K. Abadi, R. L. Vieriu, S. Winkler, and N. Sebe. "ASCERTAIN : Emotion and Personality Recognition using Commercial Sensors". In: *IEEE Transactions on Affective Computing* (2016).

[89] Y. Wu, E. V. Dijk, M. Aitken, and L. Clark. "Missed losses loom larger than missed gains : Electrodermal reactivity to decision choices and outcomes in a gambling task". In: *Cognitive, Affective & Behavioral Neuroscience* 16 (2016), pp. 353–361.

[90] C. W. Korn, M. Staib, A. Tzovara, G. Castegnetti, and D. R. Bach. "A pupil size response model to assess fear learning: Pupil responses and fear conditioning". In: *Psychophysiology* 54 (2017), pp. 330–343.

[91] D. Li, T. Liu, X. Zhang, M. Wang, D. Wang, and J. Shi. "Fluid intelligence , emotional intelligence , and the Iowa Gambling Task in children". In: *Intelligence* 62 (2017), pp. 167–174.

[92] J. A. Miranda-Correa, M. K. Abadi, N. Sebe, and I. Patras. "AMIGOS : A Dataset for Affect , Personality and Mood Research on Individuals and Groups". In: *IEEE Transactions on Affective Computing* (2017), pp. 1–14.

[93] L. I. Thompson. "Physiological Correlates of Affective Decision- Making in Anxiety and Depression". PhD thesis. City University of New York, 2017.

[94] J. Zhou, K. Yu, S. Z. Arshad, S. Berkovski, S. Luo, and F. Chen. "Indexing Cognitive Load using Blood Volume Pulse Features". In: *Conference on Human Factors in Computing Systems*. 2017, pp. 2269–2275.

[95] *biosignalsplux | wearable body sensing platform*. URL: http://www.biosignalsplux.com/index.php/en/ (visited on 10/08/2017).

[96] *Eye Tracking Solutions by SMI*. URL: https://www.smivision.com/ (visited on 05/09/2017).

[97] *hgamboa/novainstrumentation*. URL: https://github.com/hgamboa/novainstrumentation (visited on 11/08/2017).

[98] *Neurobehavioral Systems*. URL: https://www.neurobs.com/ (visited on 09/14/2017).

[99] *seaborn: statistical data visualization*. URL: https://seaborn.pydata.org/ (visited on 10/08/2017).

[100] *Welcome to Nolds' documentation!* URL: https://cschoel.github.io/nolds/ (visited on 09/14/2017).

[101] *Welcome to Python.org*. URL: https://www.python.org/ (visited on 10/08/2017).